

University of Alberta

A NOVEL ZONAL UWB RECEIVER WITH SUPERIOR PERFORMANCE

by

Hua Shao



A thesis submitted to the Faculty of Graduate Studies and Research in partial fulfillment
of the requirements for the degree of **Master of Science**.

Department of Electrical and Computer Engineering

Edmonton, Alberta

Spring 2007



Library and
Archives Canada

Bibliothèque et
Archives Canada

Published Heritage
Branch

Direction du
Patrimoine de l'édition

395 Wellington Street
Ottawa ON K1A 0N4
Canada

395, rue Wellington
Ottawa ON K1A 0N4
Canada

Your file *Votre référence*
ISBN: 978-0-494-30021-3
Our file *Notre référence*
ISBN: 978-0-494-30021-3

NOTICE:

The author has granted a non-exclusive license allowing Library and Archives Canada to reproduce, publish, archive, preserve, conserve, communicate to the public by telecommunication or on the Internet, loan, distribute and sell theses worldwide, for commercial or non-commercial purposes, in microform, paper, electronic and/or any other formats.

The author retains copyright ownership and moral rights in this thesis. Neither the thesis nor substantial extracts from it may be printed or otherwise reproduced without the author's permission.

AVIS:

L'auteur a accordé une licence non exclusive permettant à la Bibliothèque et Archives Canada de reproduire, publier, archiver, sauvegarder, conserver, transmettre au public par télécommunication ou par l'Internet, prêter, distribuer et vendre des thèses partout dans le monde, à des fins commerciales ou autres, sur support microforme, papier, électronique et/ou autres formats.

L'auteur conserve la propriété du droit d'auteur et des droits moraux qui protègent cette thèse. Ni la thèse ni des extraits substantiels de celle-ci ne doivent être imprimés ou autrement reproduits sans son autorisation.

In compliance with the Canadian Privacy Act some supporting forms may have been removed from this thesis.

Conformément à la loi canadienne sur la protection de la vie privée, quelques formulaires secondaires ont été enlevés de cette thèse.

While these forms may be included in the document page count, their removal does not represent any loss of content from the thesis.

Bien que ces formulaires aient inclus dans la pagination, il n'y aura aucun contenu manquant.


Canada

Abstract

Ultra-wideband wireless is an emerging communication technology which offers promise as a solution for high capacity short-range multiple access systems. Multiple access interference for the time-hopping ultra-wide bandwidth systems has been analyzed by many literatures in recent years, where the conventional matched filter ultra-wide bandwidth receiver is adopted as the receiver detector. However, the conventional matched filter ultra-wideband receiver is not necessarily an optimal receiver since the multiple access interference in the time-hopping ultra-wide bandwidth systems is not Gaussian distributed.

In this thesis, an ultra-wideband receiver is proposed based intuitively on the simulated probability density function of multiple access interference for the time-hopping ultra-wideband systems. The new ultra-wideband receiver dubbed the “zonal” receiver is shown to have better performance than the conventional matched filter ultra wideband receiver in multiple access interference channels with or without the presence of the additive white Gaussian noise.

Acknowledgements

I would like to deeply thank my supervisor Dr. Norman C. Beaulieu for his patient guidance, continuous encouragement, financial support, and especially for sharing with me his enthusiasm for research during this work.

I would also like to thank all the members of our *i*CORE Wireless Communication Lab. for the help on academic and technical issues.

Last but not least, I would like to thank my family for their love and long-time encouragement.

This thesis and related work was financially supported by the Alberta Informatics Circle of Research Excellence (*i*CORE).

Contents

1	Introduction	1
1.1	History of UWB Wireless	1
1.2	Overview of UWB Wireless	3
1.3	UWB Regulations	5
1.3.1	Adoption of UWB in the United States	5
1.3.2	Regulations in Asia	9
1.3.3	Regulations in the European Union	10
1.4	Literature Review	10
1.4.1	Gaussian Approximation of the Disturbance and the Adoption of the Conventional Matched Filter UWB Receiver	10
1.4.2	Invalidity of Gaussian Approximation for the Total Disturbance . .	12
1.4.3	Other Approximations of the Disturbance and New UWB Receiver Structures	14
1.5	Thesis Outline and Contributions	16
1.6	Summary	17

2	Review of UWB Systems	19
2.1	Advantages of UWB Systems	19
2.2	Single Band vs. Multiband	21
2.2.1	Pure Impulse Radio	22
2.2.2	Multicarrier UWB signals	22
2.2.3	Comparison between I-UWB and MC-UWB	24
2.3	Pulse-Shaping for Ultra-Wideband Communication Systems	24
2.3.1	UWB Signals Regulations	25
2.4	Pulse Modulation Techniques	26
2.4.1	On-Off keying(OOK)	26
2.4.2	M-ary Biorthogonal Keying Modulation (M-BOK)	26
2.4.3	Pulse Amplitude Modulation(PAM)	27
2.4.4	BPSK and QPSK modulation	27
2.4.5	Pulse Position Modulation(PPM)	27
2.4.6	Transmitted Reference Modulation (TR)	28
2.5	UWB Multiple Access Schemes	29
2.5.1	Time-Hopping for Multiple Access	30
2.5.2	Direct-Sequence for Multiple Access	30
2.6	Conventional Reception of UWB signals	31
2.6.1	Noncoherent Detection	31
2.6.2	Coherent Detection	31

2.7	Summary	33
3	Multiple Access Interference	34
3.1	System Model	34
3.2	Previous Works on Evaluating the Validity of Gaussian Approximation . . .	40
3.2.1	Evaluation Based on Characteristic Function	40
3.2.2	Evaluation Based on GQR	51
3.3	Other Approximations of the Multiple Access Interference and New Re- ceiver Designs	53
3.4	Summary	58
4	Novel Zonal UWB Receiver	59
4.1	System Models	61
4.2	Receiver Structure	62
4.3	Validity of Zonal UWB Receiver Design	71
4.4	Performance Results	74
4.4.1	Performance in pure MAI channels	76
4.4.2	Performance in mixed MAI and AWGN channels	82
4.5	Zonal Receiver Structure Design	86
4.6	Summary and Conclusions	87
5	Conclusions and Future work	88
5.1	Conclusions	89

5.2 Future Work	93
References	95

List of Tables

1.1	Signal classification principles	7
1.2	FCC regulations about the emission limits	8
1.3	Emission limits in UFZ	9
4.1	Parameters of the UWB system	75

List of Figures

3.1	Time-hopping multiple access mechanism with bit duration T_b , frame duration T_f , and chip duration T_c . The time-hopping sequence in this case is $\{1, 4, 0, 3\}$	36
3.2	BPSK modulation where bit -1 is transmitted by inverting the pulse.	37
3.3	PPM modulation where bit 1 is transmitted by shifting the pulse by a small quantity δ in time.	38
3.4	The block diagram of the conventional matched filter UWB receiver.	41
4.1	The simulated conditional probability density function (pdf) $f(r_m d_0^{(1)} = +1)$ of the amplitude of the chip correlator output $r_m = S_m + I_m$, where I_m is the MAI in m th frame, the SIR = 10 dB, and c is a constant.	66
4.2	The simulated conditional probability density functions (pdfs) $f(r_m d_0^{(1)} = +1)$ and $f(r_m d_0^{(1)} = -1)$ of the amplitude of the chip correlator output $r_m = S_m + I_m$, where I_m is the MAI in m th frame, the SIR = 10 dB, and c is a constant.	67
4.3	The block diagram of the zonal UWB receiver.	69

4.4	The transfer characteristic of the receiver chip correlator output transform.	70
4.5	The relationship between the time shift difference τ and the interference term I_m	73
4.6	The average BER versus SIR of the conventional matched filter UWB receiver, the soft-limiting UWB receiver and the zonal UWB receiver with fixed thresholds with $N_s=4$ and $N_u=4$ when only MAI is present.	77
4.7	The average BER versus SIR of the conventional matched filter UWB receiver, the soft-limiting UWB receiver and the zonal UWB receiver with adaptive thresholds with $N_s=4$ and $N_u=4$ when only MAI is present.	78
4.8	The optimal lower and upper thresholds of the zonal UWB receiver with $N_s=4$ and $N_u=4$ when only MAI is present.	81
4.9	The average BER versus SNR of the conventional matched filter UWB receiver, the adaptive threshold soft-limiting UWB receiver and the zonal UWB receiver with $N_s=4$ and $N_u=4$ when both MAI and AWGN are present.	84
4.10	The optimal lower and upper thresholds of the zonal receiver with $N_s=4$ and $N_u=4$ when both MAI and AWGN are present.	85

Acronyms

Acronyms	Definition
UWB	Ultra-Wideband
FCC	Federal Communications Commission
LPI	Low probability of interception
EIRP	Equivalent isotropically radiated power
IDA	Infocomm Development Authority
UFZ	UWB Friendly Zone
BER	Bit error rate
ML	Maximum-likelihood
PDF	Probability density function
SIR	Signal-to-interference ratio
SNR	Signal-to-noise ratio
LOS	Line-of-sight
NLOS	Non-line-of-sight
I-UWB	Impulse radio UWB

MC-UWB	Multicarrier UWB
OOK	On-off keying
M-BOK	M-ary biorthogonal keying modulation
PAM	Pulse amplitude modulation
BPSK	Binary phase-shift keying
PPM	Pulse position modulation
TR	Transmitted reference modulation
TH	Time-hopping
TH-SS	Time-hopping spread spectrum
DS	Direct-sequence
MAI	Multiple access interference
AWGN	Additive white Gaussian noise

List of Symbols

Symbol	Definition
f_L	Lower boundary of UWB bandwidth
f_H	Upper boundary of UWB bandwidth
f_C	Center frequency
t	Transmitter clock time
$s^{(k)}$	The signal of the k th user
$p(t)$	The UWB pulse
N_s	Length of repetition code
N_c	Number of chips per information bit in DS-UWB systems
T_b	Bit duration
T_f	Single frame duration
T_c	Chip duration
$\{c_j^{(k)}\}$	Time-hopping sequence for each bit of the k th user
$\{c_n^{(k)}\}$	Spreading signature sequence
$d_j^{(k)}$	The j th binary transmitted information bit of the k th user

N_u	Number of transmitters
$r(t)$	The received signal
A_k	The attenuations associated with the k th user
τ_k	The delay of the k th user
$n(t)$	White Gaussian noise process
$v(t)$	The correlation template for TH-PPM systems
$R(x)$	The autocorrelation function of the UWB pulse waveform
S	The desired signal term of the correlator output
S_m	The desired signal term of the correlator output in the m th frame
I	The interference term of the correlator output
N	The AWGN term of the correlator output
δ	The additional time shift of binary pulse position modulation
$I^{(k)}$	The interference term of the correlator output originating from the k th user
I_m	The interference term of the correlator output in the m th frame
$\phi(\omega)$	Characteristic function
$c^{(k)}(t)$	The spread signal for the k th user
$R_{k,1}(\tau), \hat{R}_{k,1}(\tau)$	The partial cross-correlation functions
$F(\cdot)$	Cumulative density function
$f(\cdot)$	Probability density function
P_e	Average probability of bit error
$P_r(\cdot)$	Probability of a certain event

Y	Total disturbance
Y_m	Total disturbance in the m th frame
$E(x)$	Expectation of x
$\text{var}(x)$	Variance of x
m_k	The value of the time uncertainty rounded to the nearest integer
α_k	The error in the integer rounding process
r_m, \tilde{r}_m	Partial decision statistics
r, \tilde{r}	Final decision statistics
t_l	The lower threshold of the zonal receiver
t_h	The upper threshold of the zonal receiver

Chapter 1

Introduction

1.1 History of UWB Wireless

About more than 45 years ago, a small group of scientists worked to develop various techniques of sending and receiving short-impulse signals between antennas. These kinds of experiments led to “impulse radio”, later dubbed UWB radio.

Contributions to UWB industry which commenced in the late 1960s were made by a number of pioneering scientists such as H. F. Harmuth at Catholic University of America, G. F. Ross and K. W. Robbins at Sperry Rand Corporation and P. V. Etten at the USAF’s Rome Air Development Center. The basic design of UWB transceiver structures were reported in Harmuth’s books and papers. At almost the same time, Ross and Robbins brought up several application areas UWB signals could be used in, including communications and radar using coding schemes, and Ross’ U.S. patent is a landmark patent in the progress of

UWB development. Etten's testing of UWB radar systems resulted in the development of system design and antenna concepts.

Since its beginnings at that time, ultra-wide bandwidth technology has traveled an interesting road from the lab, to the military, back to the lab, and finally to into commercial prototyping and implementation. Throughout its history, this technology was alternately referred to as baseband communication, carrier free communication, impulse radio, large relative bandwidth communication, non-sinusoidal communication, and video-impulse transmission. The term "UWB" was not coined until the late 1980s, when applied to this technology by the U.S. Department of Defense.

The development of UWB technology should be credited to many innovative scientists over the last 50 years. Many experiments and developments took place in the impulse radar transmission, which is the forerunner of modern UWB technology, during this period of time. There are more than 200 technical papers published in journals between 1960 and 1999 on UWB related topics and more than 100 U. S. patents issued on UWB and UWB related technology. And this work continues with many more investigators involved in this industry. Those inventions and petitions on UWB led to the landmark FCC regulations of 2002, which permit low power ultra-wideband operations for commercial development. Under such regulations, the unlicensed users can share the spectrum, which is previously assigned to other users, on a noninterference basis.

More recently, a new definition of UWB focused on the "available spectrum" was implemented by the FCC. This definition is independent of the type of technique used to

transmit the signal. Thus, the question of how can UWB coexist with other services in the assigned spectrum without causing any harmful interference becomes very imperative.

After decades of development of UWB technology, its standards are in place and the timing is right for mass commercial adoption. UWB is an exciting technology since it could access the unprecedented, unlicensed, huge amount of spectrum. The UWB industry is on the verge of market deployment.

1.2 Overview of UWB Wireless

Ultra-wideband (UWB) communication systems are those kinds of systems whose instantaneous bandwidth is much greater than the minimum bandwidth required to deliver information at a certain rate. The characteristics of UWB systems are defined by such excess bandwidth. A conventional UWB system use carrierless, short-duration (picosecond to nanosecond) pulses with a very low duty cycle, which is less than 0.5 percent, for transmission and reception of information. The duty cycle is defined as the ratio of time that a pulse is present to the total transmission time. The average transmission power in UWB communications systems is very small because of the low duty cycle. The average power is on the order of microwatts, much smaller than is the case for the narrowband transmitted signals. But since the pulse duration is very short, the peak of the instantaneous power of an individual UWB signal is relatively large. Moreover, as we all know, frequency is inversely related to time, so short-duration UWB pulses spread their energy across a very wide range of frequencies.

Within the past 40 years, the merits of UWB communication systems have spurred a growing interest in both academic and industrial institutes. Furthermore, the advances of analog and digital electronics and UWB signal theory have enabled system designers to propose some practical UWB communication systems[1]. Before 2002, UWB was relegated by regulatory bodies, such as the FCC (Federal Communication Commission) in the United States, to purely experimental work for a very long time. In 2002, the FCC decided to change the rules to allow UWB system to operate in a broad range of frequencies.

A UWB system is different from conventional wireless communications systems in the following ways:

1. The large bandwidth in UWB systems enables good time resolution for network time distribution and precision location capability.
2. The UWB systems are able to achieve robust performance in multi-path environments since short duration pulses are used to exploit more resolvable paths.
3. The low power spectral density of UWB signals can provide a low probability of intercept (LPI), which makes coexistence with existing users possible.

UWB systems are unique because of their large instantaneous bandwidth and the potential for very simple implementations. What is more, the wide bandwidth and potential for low-cost digital design enable a single system to operate in different modes as a communications device, radar, or locator. Taken together, these properties give UWB systems a clear technical advantage over other more conventional wireless transmission approaches in high multipath environments.

1.3 UWB Regulations

The interplay between the radio acts and regulations have shaped the ways different users share the limited spectrum and coexist with each other without harmless interference. The traditional allocation of spectrum doesn't fit UWB technology any more and the arrival of the new technology has reshaped the concepts of spectrum management.

1.3.1 Adoption of UWB in the United States

As wireless communication technology and science developed, research began to show that spectrum management could be more effective than simply allocating fixed narrow-band channels. Thus, regulations have appeared since 1985, which assigned blocks of nonchannelized spectrum to mobile service providers. The mobile service providers satisfy the demands of their users by spreading each of their signals over the entire allocated bandwidth. The separation of different users could be accomplished by using special digital coding and modulation techniques. The petition for the regulation of UWB began in the 1980s, and it culminated in early 2002, when the FCC adopted the regulations for UWB permitting the use of UWB signals over a huge block of spectrum between 3.1 and 10.6 GHz at power levels commensurate with those of unintentional emitters. The commercial deployment of UWB is permitted on a noninterference basis over frequency spectrum bands already occupied by existing radio services.

Management of radio frequency spectrum in the United States is shared by the FCC and the NTIA. The FCC oversees the non-Federal users, and allocates the spectrum to

commercial, private, amateur, state, and local public safety departments. The NTIA oversees the Federal users. Since UWB signals spread energy over a wide swath of spectrum, they cannot avoid both Federal and non-Federal reserved spectra. The NTIA is principally concerned with the “restricted” frequency bands that include national security and safety-of-life operations. The FCC must coordinate with the NTIA and then 3 UWB devices were granted waivers in 1999. They are as follows:

- Time Domain for through-wall imaging device
- Zircon for a “stud-finder” for rebar in concrete
- US Radar for a ground-penetrating radar.

In 2002, the First Report and Order (R&O) was adopted by the FCC on Feb. 14 and released on Apr. 22. The R&O enables the introduction of UWB technology without causing harmful interference to the incumbent users. It defines the UWB operations in terms of the following:

- UWB bandwidth. The frequency band bounded by the points that are 10 dB below the highest radiated emission, as based on the complete transmission system including the antenna. The upper boundary is designated f_H and the lower boundary is designated f_L . The frequency at which the highest radiated emission occurs is designated f_M .
- Center frequency. The center frequency, f_C , equals $(f_H + f_L) / 2$.

TABLE 1.1

Signal classification principles

Narrowband	$B_f < 1\%$
Wideband	$1\% < B_f < 20\%$
Ultra-Wideband	$B_f > 20\%$

- Fractional bandwidth. The fractional bandwidth equals $2(f_H - f_L) / (f_H + f_L)$.
- Ultra-wideband (UWB) transmitter. An intentional radiator that, at any point in time, has a fractional bandwidth equal or greater than 0.20 or has a UWB bandwidth equal to or greater than 500 MHz, regardless of the fractional bandwidth. As for the fractional bandwidth, it is defined to classify signals as narrowband, wideband or ultra-wideband according to the principles in Table 1.1.
- EIRP. Equivalent isotropically radiated power, i.e., the product of the power supplied to the antenna and the antenna gain in a given direction relative to an isotropic antenna.
- Handheld. A handheld device is a portable device, such as a lap top computer or a PDA, that is primarily handheld while being operated and that does not employ a fixed infrastructure.

The regulations permit indoor UWB systems and handheld devices. The emission limits for the indoor UWB systems and the handheld devices are shown in Table 1.2.

TABLE 1.2

FCC regulations about the emission limits

Frequency (MHz)	Indoor EIRP (dBm)	Handheld EIRP(dBm) (dBm)
Below 960	Section 15.209	Section 15.209
960 - 1,610	-75.3	-75.3
1,610 - 1,990	-53.3	-63.3
1,990-3,100	-51.3	-61.3
3,100-10,600	-41.3	-41.3
above 10,600	-51.3	-61.3

TABLE 1.3

Emission limits in UFZ

Frequency (MHz)	EIRP (dBm)
Below 960	Not intentional
960 - 1,610	-75.3
1,610 - 1,990	-63.3
1,990-2,200	-61.3
2,200-10,600	-35.3
above 10,600	-41.3

1.3.2 Regulations in Asia

Although researchers in China, Korea, Japan, Singapore and many other Asian countries are showing their interests in UWB industry, now in Asia, only the Infocomm Development Authority (IDA) in Singapore permits UWB with a special experimental license. The UWB Friendly Zone (UFZ) in Singapore is located in Science Park II. The emission limits in UFZ are given in Table 1.3.

The emission regulation above are measured in a resolution bandwidth of 1 MHz using an RMS detector with a video integration time of 1 ms or less. The limits have an expanded lower frequency band edge than what is permitted by the FCC.

1.3.3 Regulations in the European Union

The European Technical Standards Institute (ETSI) deals with the technical standards and compatibility studies concerning the UWB technology. Its attitude towards UWB technology is more conservative than the U.S., and the proposed draft for the emission standards is significantly more restrictive than the FCC regulations. The proposed indoor emission limit of the ETSI is the same as the FCC handheld limit, while the ETSI handheld proposal is as much as 20 dB more restrictive.

1.4 Literature Review

1.4.1 Gaussian Approximation of the Disturbance and the Adoption of the Conventional Matched Filter UWB Receiver

A time-hopping spread-spectrum (TH-SS) system transmits signals occupying an extremely large bandwidth, which is much larger than the data modulation bandwidth and thus with a reduced power spectral density. The use of TH-SS impulse radio in UWB systems is motivated by the TH-SS impulse radio's ability to resolve multipath and the availability of technology to implement and generate UWB signals with relatively low complexity.

In [3], Win and Scholtz's (2000) used the TH-SS impulse radio in UWB systems. A feasible modulation scheme which can be supported by the technology at that time was described and then the receiver structure and processing was presented in this work. Under the ideal multiple-access interference channel, the performance of both analog and digi-

tal data modulation formats were predicted. The digital data modulation in this work is the same as the modulation scheme referred to as the time-hopping pulse position modulation (TH-PPM), and the receiver dubbed “Digital Impulse Radio Multiple-Access Receiver (DIRMA)” is based on the theory of hypothesis testing for fully coherent detection. It was also mentioned in [3] that the decision rule for this receiver is no longer optimal with the presence of multiple access interference which is not really Gaussian distributed, and an optimal receiver design should use information of the statistics of the multiple access interference. However, since the optimal receiver for the multiuser systems is not feasible, [3] adopted the Gaussian approximation for the total disturbance and employed the DIRMA as an optimal receiver structure based on the approximation. Although the assumption is not strictly valid, the DIRMA is a good suboptimal means of making data decisions because it is simple and it suggests practical implementations. Ramirez-Mireles’s (2001) work [11] extended the case to non binary PPM schemes, but it still modeled the multiple access interference as a Gaussian random process.

Taha and Chugg’s (2002) work [13] used the modulation scheme of TH-BPSK. The whole UWB system was mathematically modelled. The SNR and bit error rate in the presence of arbitrary random wide-sense stationary external interference was computed. When it came to the bit error rate computation, the central limit theorem was applied and the Gaussian approximation was adopted. The receiver structure in this work was also based on coherent detection and the conventional matched filter UWB receiver was adopted. The bit error rate was predicted in such receiver structures.

1.4.2 Invalidity of Gaussian Approximation for the Total Disturbance

Studies of multiple access interference for time-hopping UWB systems have been conducted in recent years. The Gaussian approximation for the total disturbance was firstly introduced and the conventional matched filter UWB receiver was adopted in systems as the optimal receiver structure based on the assumption that the total disturbance is Gaussian distributed. However, it was shown in many literatures that the multiple access interference is not Gaussian distributed, and the Gaussian approximations highly underestimate the bit error rate performance of UWB systems for medium and large SNR values.

The multiple access interference in TH-PPM systems was studied in [14]. It was assumed in this work that the overall disturbance, including MAI and AWGN, was a zero mean Gaussian random process. The conventional matched filter UWB receiver was adopted and an analytic expression for the bit error rate was obtained. The analytic results for the BER based on the Gaussian approximation were compared with the ones derived from simulation. It is obvious to note the extremely limited capacity of the Gaussian approximation to describe the real performance of TH-PPM techniques, especially when the slot duration T_c is much larger than the pulse duration T_p . Thus, it is not reasonable to model the statistical characteristics of the total disturbance as a Gaussian zero mean random process and the conventional matched filter UWB receiver is not necessarily an optimal receiver for UWB systems.

Another important analysis concerning the performance evaluation of TH-PPM UWB systems in the presence of multiuser interference was revealed in [15]. It was mentioned in

this work that the Gaussian approximation is not accurate enough to predict the BER performance of UWB systems. Compared with the BER performance obtained using Gaussian approximation, the simulation results showed that the Gaussian approximation may significantly underestimate the BER of UWB systems. A new method to evaluate the BER performance of TH-PPM systems in the presence of MAI and AWGN channel was proposed in this work, which was based on Gaussian quadrature rules (GQR). This technique can overcome the problem of evaluating the exact pdf of the multiuser interference, which was proved in [16] to be very cumbersome. The technique proposed in this work requires only estimation of the moments of the MAI, and it is able to predict the BER performance of TH-PPM systems with necessary accuracy with limited computational complexity. The results showed that the BER performances obtained by the GQR techniques perfectly agree with the simulation results, which confirmed the accuracy of the proposed method. It was also showed in this work that the Gaussian approximation highly underestimates the BER performance of the TH-PPM systems.

In [17]- [19], the statistics of the multiple access interference has been studied more systematically. An exact analysis was derived for precisely calculating the bit error rate for both time-hopping (both TH-BPSK and TH-PPM) and direct-sequence (DS) UWB systems in multiple access interference channels. Theoretical expressions for the bit error rate in TH-BPSK, TH-PPM, and DS-BPSK UWB systems were obtained in their work, and the accuracy of these expressions was confirmed by simulation results. The theoretical results were then used to test the validity of Gaussian approximation of the total disturbance. It

was shown that the Gaussian approximation is invalid to describe the statistics of the total disturbance when multiple access interference is present in the channel, and the Gaussian approximation highly underestimates the bit error rate performance for medium and large values of SNR in UWB communications systems. Meanwhile, it was seen in their work that the Gaussian approximation led to some contradictions about the bit error rate performance of UWB systems. According to predictions obtained using the Gaussian approximation, TH-BPSK systems outperform DS-BPSK systems, whereas the theoretical results in their work showed that the DS-BPSK systems' bit error rate performances surpass those of the TH-BPSK systems for medium and large SNR values.

1.4.3 Other Approximations of the Disturbance and New UWB Receiver Structures

Since the Gaussian approximation for the total disturbance is invalid, the conventional matched filter UWB receiver which was originally introduced and widely used in UWB systems is not necessarily the optimal UWB receiver. Some other approximations of the statistics of the total disturbance were introduced, and new receiver structures based on the new approximation have been proposed. The performances of the new receiver structures were shown to surpass the widely-used correlation (conventional matched filter) UWB receiver in multiple access interference channels.

Note that the Laplace noise model is used to characterize impulsive noise and the short bursts of multiple access interference in UWB systems are impulse-like, so the Laplacian

approximation of the total disturbance is then adopted. The optimal detection procedure considering additive noise whose statistics are Laplacian was derived in [22]. The ML receiver principle was used and an optimal processor for the Laplacian noise model was obtained. Later in [23], the discrete-time detection of time-varying, additive signals in independent Laplace noise was considered, and the Neyman-Pearson optimal detector for the signal embedded in Laplacian noise was proposed. Beaulieu and Hu use this optimal Laplacian receiver in TH-UWB systems for the first time and a new UWB receiver dubbed the soft-limiting UWB receiver was proposed in [24]. The soft-limiting UWB receiver achieves as much as 10 dB gain when only multiple access interference is present in the channel. In more practical multiple access interference plus AWGN channels, it underperforms the conventional matched filter for small to moderate values of SNR, but achieves more than 1 dB gain for practical moderate and large values of SNR. An adaptive version based on the soft-limiting UWB receiver was proposed later [25], and this new receiver structure always meets or outperforms the conventional matched filter UWB receiver for all values of SNR when both MAI and AWGN are present in the channel.

The use of the soft-limiting receiver structure is intuitive since the distribution of the multiple access interference is still unknown. Thus, there is no reason to believe that the soft-limiting UWB receiver is the optimal receiver for UWB systems. Actually, if we want to find the optimal receiver for UWB systems, the distribution of the multiple access interference should be studied and the ML receiver principles should be applied to get the receiver structure. However, characterizing mathematically the pdf of the multiple access

interference seems difficult and it is not tractable to derive rigorously an optimal receiver design using ML receiver design principles. Still, a better receiver can be derived based on some observations on the pdf of the multiple access interference, and this is the motivation of our new receiver structure design.

1.5 Thesis Outline and Contributions

This thesis will intuitively propose a new UWB receiver dubbed the “zonal” receiver. Firstly, the simulated probability density function of the total disturbance including multiple access interference and additive white Gaussian noise in the UWB systems will be analyzed and a new receiver structure will be derived based on observations of the characteristics of the pdf for the total disturbance. The superiority of the new UWB receiver will be shown by simulation results. The new UWB receiver structure outperforms both the conventional matched filter UWB receiver and the soft-limiting UWB receiver when only multiple access interference is present in the channel. In more practical multiple access interference-plus-noise environments, the new receiver structure’s bit error rate performance always surpasses that of the conventional matched filter UWB receiver, and it outperforms the adaptive threshold soft-limiting UWB receiver for large values of SNR.

Chapter 2 reviews the overall situation of UWB systems. In this chapter, the advantages of UWB systems over traditional narrowband communication systems will be summarized. Two forms of UWB signals, the standard impulse radio UWB signals and the multicarrier UWB signals are going to be discussed and compared with each other. Since

modulation schemes and pulse-shaping are important in UWB systems, these contents will also be included in Chapter 2. Last but not least, conventional reception of UWB signals will be briefly introduced, which is closely related to our work about UWB systems.

The multiple access interference, which is the main concern of our work, will be discussed in Chapter 3 in detail. Previous works on this topic will be reviewed and interesting and important conclusions will be recalled in this chapter. Some of the conclusions which lead to our motivations for the new UWB receiver design will be discussed.

In Chapter 4, system models for time-hopping UWB wireless will be recalled and the general mathematical close forms of the correlator output are going to be developed. Some interesting phenomena about the pdf of the output correlator can be observed and the new UWB receiver will be derived based on them. Simulation results will be used to show the superiority of the new receiver.

Chapter 5 concludes the results and achievements of the thesis. Problems which will merit the future research are also going to be proposed in this chapter.

1.6 Summary

In this chapter, the history of UWB wireless communications has been briefly described and overviewed, and new regulations on the UWB technology in the United States, Asia, and Europe have been introduced, respectively. Since our work focuses on the receiver side of the UWB systems, some important literatures related to the UWB receivers and the BER performances of the receivers are also studied and reviewed in this chapter. This chapter is

ended with the outline of the thesis and the contributions that it makes.

Chapter 2

Review of UWB Systems

2.1 Advantages of UWB Systems

UWB signals have the ability to share the frequency spectrum with narrowband signals. As mentioned above, the FCC spectral emission requirement for UWB signals is that the radiated emission shall not exceed the average limits of -41.3 dBm when measured using a resolution bandwidth of 1 MHz, which means that the signal power spectral density can not exceed 75 nanowatts/MHz. This restriction puts UWB signals fall below the noise floor of typical narrowband signals. Thus, UWB can coexist with current radio services without harmful interference.

One of the most major advantages of the UWB systems is the improved channel capacity. According to the Hartley-Shannon capacity formula, the capacity of a communications

channel is given by [26]

$$C = B \log_2(1 + \text{SNR}) \quad (2.1)$$

where C is the maximum channel capacity, B is the channel bandwidth, and SNR is the signal-to-noise ratio. Observe that the maximum channel data rate increases linearly with the bandwidth B . Since the bandwidth of UWB systems is on the order of gigahertz, UWB systems can provide large channel capacity. The current power limitation on UWB transmissions make the high data rate only available for short ranges. This makes the UWB systems perfect candidates for short-range, high-data-rate wireless applications. The trade-off between the communications range and the data rate make the UWB technology ideal in a wide range of sections, such as military, civil and commercial areas. The Hartley-Shannon formula also shows that the capacity of the channel depends only logarithmically on the SNR . Thus, even in harsh communication channels where the SNR is small, UWB systems can still offer large channel capacity because of their large bandwidth.

The small average transmission power of UWB systems makes it very hard for the eavesdroppers to detect the transmitted information. Therefore, the UWB communication systems have high immunity to detection and interception. In addition, the UWB signals are time modulated with codes which are unique to each transmitter/receiver pair. The extremely narrow pulses make the UWB even more secure since the detection of picosecond pulses without any knowledge of the arrival time is next to impossible. Thus, UWB systems can be designed to achieve high security, which is critical to military use.

The low duty cycle of UWB signals can also bring other benefits to UWB systems. The

effect of multipath caused by the multiple reflection of transmitted signals from various surfaces is rather severe for narrowband signals, and it can cause up to -40 dB signal degradation due to the out-of-phase addition of LOS and NLOS waveforms. However, the low duty cycle and the short duration of the UWB pulses make the UWB signals less sensitive to multipath effects. In most cases, the pulse duration is on the order of nanoseconds and it gives a very short time window for the reflected pulse to collide with the LOS pulse and cause a degradation.

As mentioned before, the standard UWB signals are carrierless; this means that the transmitter doesn't have to translate the transmitted signals to a higher frequency, which means that few RF components are required in UWB systems than the conventional carrier-based transmission. For example, there is no need for mixers and local oscillators to translate the carrier recovery stage at the receiver end. Therefore, the architectures of the transmitter and the receiver in UWB systems can be simple and cheaper to build.

2.2 Single Band vs. Multiband

There are two common forms of UWB, one based on sending very short duration pulses to convey information, and referred to as the standard UWB, the other approach, which in contrast to standard UWB, uses carriers in an orthogonal frequency division multiplexing implementation (OFDM). The single-band techniques, backed by Motorola/XtremeSpectrum, supports the idea of impulse radio which is the original approach to UWB by using short-duration pulses that occupy a large swath of bandwidth. The multiband approach, which

is supported by several other companies, including Staccato Communications, Intel, Texas Instruments, General Atomics, and Time Domain Corporation, divides the available UWB bandwidth into slots of spectrum with bandwidths greater than 500 MHz [2]. This approach has its relative technical merits because OFDM has become the leading modulation for high data rate systems, and much information on this modulation type is available in recent technical literature.

2.2.1 Pure Impulse Radio

Unlike classic communications, pure impulse radio transmits information without translating it to a higher frequency, thus it is called carrierless impulse radio. The transmitted signal is a series of baseband pulses. Since the pulses are extremely short (commonly in the nanosecond range or shorter), the transmitted signal bandwidth is on the order of gigahertz or the fractional bandwidth is greater than 20%. Impulse radio UWB promises simplicity, low cost, low power consumption, and superior multipath rejection. All these characteristics make the impulse radio UWB suitable for a broad range of communications, positioning, and radar imaging applications.

2.2.2 Multicarrier UWB signals

Multicarrier communications were first used in the late 1950s and early 1960s for higher data rate HF military use. Subsequently, OFDM emerged as a special case of multicarrier modulations. However, OFDM was not practical until some innovations occurred.

First, OFDM needs precisely overlapping but noninterfering subcarriers, which requires a real-time Fourier transform operation. Improvements in VLSI led to the real-time Fourier transform becoming feasible. There are other issues in OFDM implementation, such as oscillator stability and compensation of channel effects as well as Doppler spreading caused by rapid time variations of the channel which can cause interference between carriers .

OFDM is now used in many cases, such as ADSL, DAB, DVB in Europe, ISDB in Japan, IEEE 802.11 a/g, 802.16a, and Power Line Network(HomePlug). The fourth generation(4G) wireless services and IEEE 802.11n and IEEE 802.20 are also considering adopting OFDM since it is suitable for high rate data systems.

The basic concept behind multiband OFDM divides the spectrum into subchannels which have bandwidth of 528 MHz, since each of the subchannel occupies more than 500 MHz for all the transmission time, it obeys the UWB regulations of the FCC. This communications method takes advantage of frequency diversity and has necessary robustness against interference and multipath. A multiband OFDM system's architecture is similar to other conventional OFDM systems. It benefits a lot since OFDM has been widely accepted by other standard organizations.

The multicarrier UWB baseband signal model is

$$s(t) = \sum_{i=-\infty}^{+\infty} d_i(t) e^{j2\pi i(T/T_s)} \quad (2.2)$$

where $T_s = NT_b$ is the symbol duration, and $d_i(t)$ is the data symbol stream modulating the i th subcarrier.

2.2.3 Comparison between I-UWB and MC-UWB

I-UWB and MC-UWB systems have their own merits and demerits respectively. When the particularly important issue of how to minimize the interference transmitted and received by UWB systems is considered, MC-UWB systems work quite well since their carrier frequency can be precisely chosen to avoid the narrowband interference. But such systems need an extra layer of control in the physical layer. What is more, continuous variations in power over a very wide bandwidth will complicate the implementation of MC-UWB systems. For example, in an OFDM system, high-speed FFT processing is necessary, requiring significant processing power.

As for I-UWB systems, high precise synchronization is required. The transmitter and receiver of such systems need fast switching times. Since the impulse duration is very short, the instantaneous power during the brief interval is good for the signal to overcome the interferences from UWB systems, but it can easily interfere with the transmission in the narrowband systems. I-UWB systems also have merits, they are very simple and inexpensive to construct.

2.3 Pulse-Shaping for Ultra-Wideband Communication Systems

In UWB systems, pulse-shaping is very important since it will strongly affect the spectral emission, the design of filters, the choice of receiver bandwidth and the bit error rate per-

formance. UWB signals should spread the energy as widely in frequency as possible so the power spectral density (PSD) is as small as possible, and the interference to other users is minimized.

2.3.1 UWB Signals Regulations

The regulations for UWB systems have shaped the characteristics of UWB signals. The UWB systems must operate in the frequency bandwidth 3.1 GHz to 10.6 GHz. Moreover, the device must be designed to ensure that the operation can only occur indoors or it must be designed for peer-to-peer operation using handheld devices. International UWB radiators must be designed to guarantee that the 20-dB bandwidth must be contained in the UWB frequency band. The bandwidth measured at 10 dB below the peak emission level should be at least 500 MHz. The maximum emission level for UWB signals in the UWB band is set at -41.3 dBm/MHz.

A variety of pulse shapes has been proposed for UWB systems. A set of Gaussian monocycles were originally proposed for UWB communications systems and now have been widely adopted in UWB applications, and then the Manchester monocycle was proposed for UWB systems [4], which is designed to approach an ideal transmission power spectrum and avoid DC component. An orthogonal pulse set was proposed by [5], and the pulse design is based on modified Hermite polynomials (HP). A pulse design algorithm utilizing the concepts of prolate spheroidal (PS) functions was proposed by [6]. And more recently, a novel pulse design paradigm for ultra-wideband communication systems was

proposed by [9]. The average bit error rate of time-hopping UWB systems employing the different pulses which can meet the FCC regulations (possibly with frequency translation) are examined and compared in [10].

2.4 Pulse Modulation Techniques

2.4.1 On-Off keying(OOK)

On-off keying is the simplest kind of modulation, in which data bit 1 is represented by a UWB pulse while 0 is represented by the absence of the pulse. The OOK signal is

$$s(t) = \sum_{m=1}^M b_m \cdot P(t - T) \quad (2.3)$$

where $P(t)$ is the UWB pulse, b_m is the data bit, which assumes a value of 0 or 1, and M is the maximum number of transmitted bits. OOK modulation's main advantages are simplicity and low implementation cost, but it is very sensitive to noise and interferences.

2.4.2 M-ary Biorthogonal Keying Modulation (M-BOK)

M-ary biorthogonal keying modulation is a combination of clever coding with pulse polarity. In this modulation scheme, N moderate length codes correspond to M symbols. If the set only consists of 2 codes, the modulation scheme works the same as BPSK, while when the code length is long, the chip sequence acts as a direct-sequence spreading code.

2.4.3 Pulse Amplitude Modulation(PAM)

Pulse amplitude modulation encodes the data bits on different levels of amplitude. Two level PAM, or 2-PAM, works the same as the 2-BOK modulation scheme. However, as M increases, the modulation becomes more fragile and requires higher SNR per bit. Although PAM are less sensitive to noise in the communication channel than OOK, the attenuation in the channel can effectively convert it into the latter modulation scheme. Thus, it has the same disadvantages as OOK.

2.4.4 BPSK and QPSK modulation

Transmission of an information bit sent individually with polarity modulation is the same as the BPSK modulation in conventional carrier-based signaling. It works the same as the 2-BOK and 2PAM. In a QPSK modulation scheme for UWB signals, impulses can also be designed to be orthogonal to each other, then these can may be superimposed in time and frequency to form a modulation scheme which is equivalent to conventional QPSK modulation.

2.4.5 Pulse Position Modulation(PPM)

PPM modulation has been developed in the form of time modulation (TM) and was introduced at the end of 1980s by Time Domain Corporation. The pulses of this modulation scheme are not necessarily evenly spaced in time domain. Actually, the signals are pseudorandomly encoded based on the position of the transmitted pulse trains by shifting the

pulses in a predefined window in time. A version of PPM presents 0 by no shift and 1 by a certain shift with respect to a specific reference point in time.

This modulation scheme creates a noiselike signal in both the time and frequency domains. UWB systems adopting this modulation technology with low power levels have demonstrated impressive position measurements in both short and long-range data links, which can be precise to a few centimeters. Pulse position modulation UWB signals are less sensitive to the channel noise than PAM signals, but they are vulnerable to the catastrophic collisions caused in multiple access interference channels.

2.4.6 Transmitted Reference Modulation (TR)

Transmitted reference (TR) modulation offers different advantages than the modulation schemes above, and it has been playing an increasingly important role in UWB systems. This modulation scheme employs differentially encoded impulses sent at a precise spacing D . TR modulation signals consists a pair pulses or doublets where the first one is the reference pulse and the second one is the data pulse. Each pulse here can be any kind of wideband pulse. At the receive side, the pulses, including propagation induced multipath replicas, are detected using a self-correlator with one input fed directly and another input delayed by the spacing D .

An important advantage of TR modulation is that it sends the same signals twice through the unknown channel. Both pulses experience the same type of channel distortion, thus, detection with a correlation receiver becomes easier. TR modulation works quite

well in multipath environments since the reference and data pulses are correlated with each other.

TR modulations also have disadvantages. First, this kind of modulation can suffer from a major drawback caused by the overlap of the reference and data pulses in certain channels. Second, for every data bit, the system should send it twice, and consequently the data rate is slower. Furthermore, although a TR receiver doesn't need strict synchronization, its performance depends largely on its integration window.

2.5 UWB Multiple Access Schemes

UWB technology can deliver a large amount of information data with low power spectrum density. In UWB applications, several transmitters should coexist in the same covered area. The received signal in such systems is the superposition of all the signals in the same channel, with different attenuations and delays. A major factor in the multiuser receiver is the multiple access interference (MAI). It is caused by the unwanted signals in the same channel. The effect of MAI is quite severe in UWB systems because of the transmit power restriction. Certain multiple access techniques can be adopted to eliminate MAI. Thus, multiple access schemes have drawn significant research interest. Various multiple access schemes and their performance have been reported in [3], [12]. Time-hopping (TH) and direct-sequence (DS) have proved to be two attractive methods for multiple access in UWB systems.

2.5.1 Time-Hopping for Multiple Access

There are various modulation schemes available for TH-UWB systems, such as TH-PAM and TH-PPM, which will later be explained in detail. As mentioned in previous chapters, the duty cycle of UWB signals is small and the transmitter is gated off for a large portion of a symbol period. In time-hopping, one divides the time frame T_f into subunits called chips with duration T_c and appropriately assign a unique hopping sequence to each user to avoid catastrophic collisions due to multiple access. Certain additional time shifts based on each user's hopping sequence will be added to diminish the MAI. In a TH-PPM scheme, information bits are carried by the absence and presence of the additional time shift δ , while in TH-PAM systems, information bits are transmitted by changing the amplitude of the time-hopped pulse. The general mathematical signal model of TH-PPM and TH-BPSK (which is a special case for TH-PAM) can be expressed as

$$s_{\text{PPM}}^{(k)}(t) = \sqrt{\frac{E_b}{N_s}} \sum_{j=-\infty}^{+\infty} p\left(t - jT_f - c_j^{(k)}T_c - d_{\lfloor j/N_s \rfloor}^{(k)}\delta\right) \quad (2.4)$$

and

$$s_{\text{BPSK}}^{(k)}(t) = \sqrt{\frac{E_b}{N_s}} \sum_{j=-\infty}^{+\infty} d_{\lfloor j/N_s \rfloor}^{(k)} p\left(t - jT_f - c_j^{(k)}T_c\right) \quad (2.5)$$

respectively. The notations and terminologies will be explained in the following chapter.

2.5.2 Direct-Sequence for Multiple Access

Direct-sequence has also proved to be a useful scheme for multiple access in UWB systems.

This scheme can be used in various modulation methods such as PAM and PPM. In this

multiple access technique, spreading codes are used for accommodating multiple users, and each symbol is represented by a series of pulses that are pulse-amplitude-modulated by a chip sequence. The transmitted waveforms carry the useful information either in the amplitude (DS-PAM) or in the relative positions (DS-PPM) of each sequence of pulses.

2.6 Conventional Reception of UWB signals

2.6.1 Noncoherent Detection

Noncoherent detection use energy detectors which detect the energy of a signal and demodulate the signal by comparing it to a threshold level. The noncoherent detection in UWB systems uses the same principle as the noncoherent detection in conventional narrowband communication systems. The noncoherent receiver consists of a squaring device, followed by a finite integrator and a decision threshold comparator. Once the transmitted signal reaches the receiver, its energy is calculated by the squaring device. This energy passes through the detector and then the information bit is demodulated based on the threshold.

2.6.2 Coherent Detection

Detecting a UWB signal coherently is a matter of matching the received energy to a pre-determined template. This technique is a mathematical operation measuring the similarity between two signals, and it is widely used in all types of pattern-recognition and signal-processing problems. Coherent detection was originally introduced and widely used in the

detection of UWB signals. If we know the expected shape of the signal and when the signal is expected at the receiver side, the shape and time are matched. In coherent detection, a classical matched filter is adopted. It performs a correlation operation on the received signal, $r(t)$, which comprises the transmitted signal and the noise term. The classical matched filter maximizes the received signal's SNR when the signal is corrupted by AWGN [28]. However, if the signal is corrupted by other forms of disturbances, such as multiple-access interference (MAI) or narrowband interference (NBI), which do not have AWGN statistics, the classical matched filter is not necessarily optimal.

The following equations show the matched filter's suboptimal performance in a two-user system where the received signal, $r(t)$, consists of user one's signal, $s_1(t)$, user two's signal, $s_2(t)$, and random noise in the channel, $w(t)$,

$$r(t) = s_1(t) + s_2(t) + w(t). \quad (2.6)$$

Assume that the signal from user one s_1 is the desired signal. Then the matched filter will multiply the received signal by $s_1(t)$ and integrate the product over a finite time.

$$\hat{s}_1 = \int_0^T [s_1(t) + s_2(t) + w(t)] \cdot s_1(t) dt \quad (2.7)$$

$$\hat{s}_1 = \underbrace{\int_0^T s_1^2(t) dt}_{E_p} + \underbrace{\int_0^T s_2(t) \cdot s_1(t) dt}_{MAI} + \underbrace{\int_0^T w(t) \cdot s_1(t) dt}_0. \quad (2.8)$$

In eq. (2.8), the first term is useful signal energy. The second term is the correlation between the desired signal and the unwanted signal, known as multiple access interference. It can not be ignored and will seriously damage the performance of the conventional matched filters in multiple access systems. So modulation schemes should attempt to minimize

the overlap of unwanted signals with the desired signal to make the conventional matched filters perform better. This is the purpose of time-hopping or direct-sequence in UWB systems. The third term in eq. (2.8) is receiver noise unrelated to multiple access interference and is well modelled as Gaussian noise. Note that the second term in eq. (2.8), the multiple access interference does not have Gaussian statistics which is shown by many literatures recently. If an optimal receiver is to be designed to replace the conventional matched filter UWB receiver, which is not necessarily an optimal receiver for UWB systems, the statistics of the total disturbance should be studied and then the ML receiver design principles can be used to get the optimal receiver structure.

2.7 Summary

In this chapter, the overall situation of UWB systems has been reviewed. Firstly, the advantages of UWB systems were introduced. Then, two different forms of UWB signals, impulse radio and multicarrier UWB signals, were briefly described. Pulse-shaping and UWB signal regulations were also included in this chapter because the pulse-shaping is important and it strongly affects the spectral emission, the design of filters, the choice of receiver bandwidth and the bit error rate performance. Later, several modulation scheme and UWB multiple access schemes, which are used to avoid the catastrophic collisions between different users, were briefly described. Last but not least, conventional detection of UWB signals, including noncoherent detection and coherent detection, were discussed.

Chapter 3

Multiple Access Interference

3.1 System Model

In this chapter, the characteristics of multiple access interference of UWB systems will be studied. We only consider two widely used UWB systems, the asynchronous TH-PPM and TH-BPSK. These UWB systems have been described and studied in many literatures. The same notation and terminology are used here and a unified framework is introduced [3], [13].

As mentioned in previous chapter, in a time-hopping UWB system, each bit duration T_b is divided into N_s disjoint frames with duration of T_f . In each frame, a UWB waveform is placed with its position being chosen randomly inside the frame. A frame is further divided into N_h chips with duration of T_c . Each user is assigned a unique time-hopping code $\{c^{(k)}\}$ with each $c^{(k)}$ uniformly distributed in $[0, \dots, N_h - 1]$, and the position of the waveform in

each frame is decided by the time-hopping sequence. The time-hopping multiple access mechanism is illustrated in Fig. 3.1.

Two commonly used modulation schemes with time-hopping UWB systems are BPSK and PPM. In BPSK systems, the pulse corresponding to a 1-bit remains unaltered, while a -1-bit is represented by the inverted pulse. In a PPM scheme, 0 is expressed by a unaltered pulse, while the pulse corresponding to a 1-bit is shifted in time by a small quantity δ . The BSPK and PPM schemes are illustrated in Fig. 3.2 and Fig. 3.3, respectively.

Thus, a TH-PPM UWB signal has the form

$$s_{\text{PPM}}^{(k)}(t) = \sqrt{\frac{E_b}{N_s}} \sum_{j=-\infty}^{+\infty} p\left(t - jT_f - c_j^{(k)}T_c - d_{\lfloor j/N_s \rfloor}^{(k)}\delta\right) \quad (3.1)$$

and a TH-BPSK UWB signal is represented as

$$s_{\text{BPSK}}^{(k)}(t) = \sqrt{\frac{E_b}{N_s}} \sum_{j=-\infty}^{+\infty} d_{\lfloor j/N_s \rfloor}^{(k)} p\left(t - jT_f - c_j^{(k)}T_c\right) \quad (3.2)$$

where t is the transmitter clock time, and $s^{(k)}(t)$ is the signal of the k th user. The function $p(t)$ is the transmitted UWB pulse which takes forms of the arbitrary pulse shapes proposed for UWB systems, such as the Beaulieu-Hu pulses [9], the Gaussian monocycles, the modified Hermite polynomial based pulses and the prolate spheroidal functions-based pulses. The pulse function is normalized to have unit energy, i.e. $\int_{-\infty}^{+\infty} p(t) dt = 1$. Other notations are as follows:

- E_b is the bit energy, and N_s is the number of frames used to transmit a single information bit, which can also be referred to as the length of repetition code. The term $\sqrt{E_b/N_s}$ is the normalization factor which assures that all the systems have the same

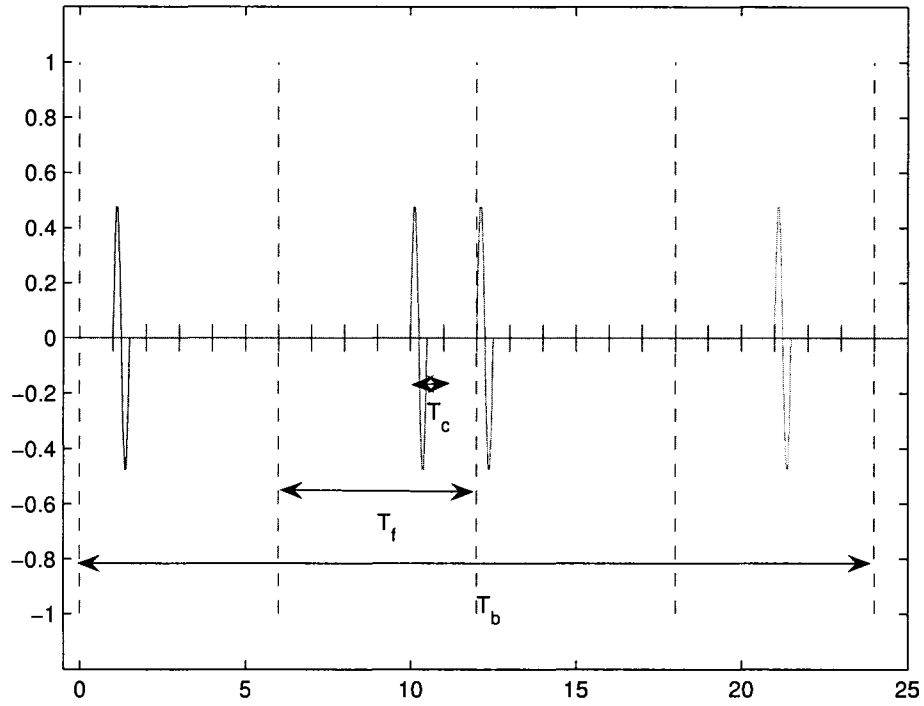


Fig. 3.1. Time-hopping multiple access mechanism with bit duration T_b , frame duration T_f , and chip duration T_c . The time-hopping sequence in this case is $\{1, 4, 0, 3\}$.

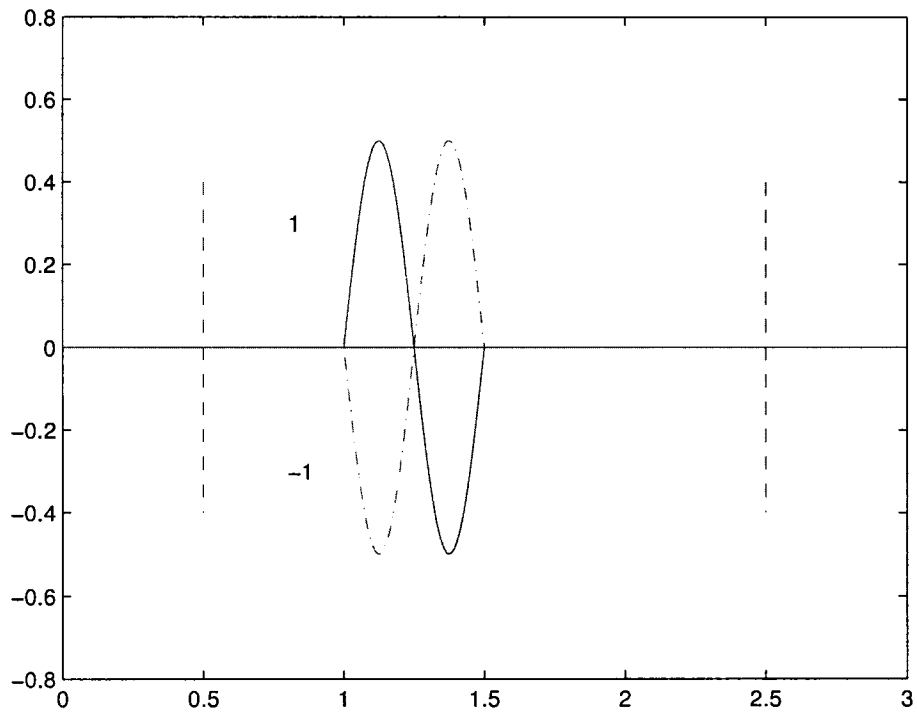


Fig. 3.2. BPSK modulation where bit -1 is transmitted by inverting the pulse.

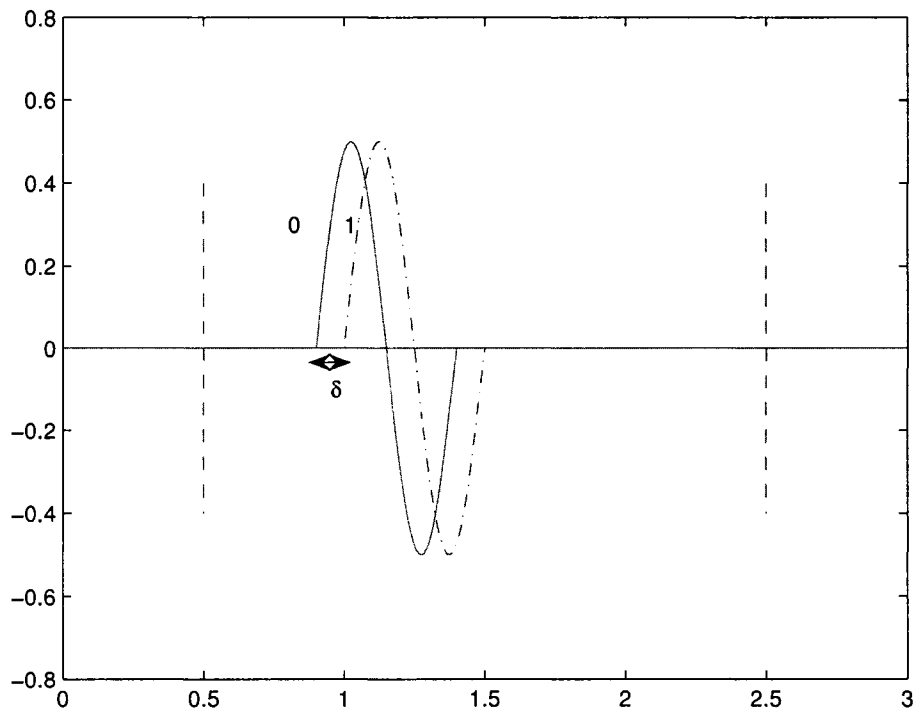


Fig. 3.3. PPM modulation where bit 1 is transmitted by shifting the pulse by a small quantity δ in time.

energy per bit, E_b .

- T_f is the duration of a single frame, which is divided into hop width with duration T_c in the TH-UWB systems. The hop width in TH-UWB systems satisfies the condition $N_h T_c = T_f$, where N_h is the number of hops.
- The sequence $\{c_j^{(k)}\}$ is the time-hopping sequence for each bit of the k th user which takes integer values in the range $0 \leq c_j^{(k)} < N_h$. The product $c_j^{(k)} T_c$ represents an additional time shift added to the TH pulses to avoid catastrophic collisions.
- In the TH-UWB systems, the bit duration T_b satisfies the condition $T_b = N_s T_f$.
- The j th binary transmitted information bit of the k th user is represented by the notation $d_j^{(k)}$. In the TH-PPM systems, $d_j^{(k)}$ takes values in $\{0, +1\}$, while in the TH-BPSK it assumes values in $\{-1, +1\}$.

Assuming ideal free-space propagation for clarity, when there are N_u transmitters in the same coverage area, the received signal can be written as

$$r(t) = \sum_{k=1}^{N_u} A_k s^{(k)}(t - \tau_k) + n(t) \quad (3.3)$$

where the amplitudes $\{A_k\}_{k=1}^{N_u}$ are the channel attenuations associated with the users. The random variable τ_k , for $k = 1, 2, \dots, N_u$, is the delay of the k th user which can be assumed to be uniformly distributed on $[0, T_b)$, and $n(t)$ is a white Gaussian noise process with two-sided power spectral density $N_0/2$.

3.2 Previous Works on Evaluating the Validity of Gaussian Approximation

The coherent detection was originally introduced in UWB systems and the conventional matched filter is widely adopted as the UWB receiver. However, the conventional matched filter is only optimal when the signal to be recovered is corrupted by additive white Gaussian noise [28]. Since there is no evidence showing that the total disturbance in UWB systems is Gaussian distributed, the conventional matched filter is not necessarily the optimal UWB receiver. Evaluation of the validity of Gaussian approximation for the total disturbance will help to answer the question whether the conventional matched filter UWB receiver is the optimal receiver for UWB systems or not.

3.2.1 Evaluation Based on Characteristic Function

Evaluating mathematically the true pdf of MAI in UWB systems seems to be difficult. Several other methods have been proposed to evaluate the BER performance of UWB systems and the validity of Gaussian approximation for the total disturbance. An exact analysis was derived for precisely evaluating the BER performance for time-hopping and direct-sequence UWB systems in [19]. In this work, correlation detection of the UWB signals was adopted. In the correlation detection process, a correlation template $v(t)$ is adopted by the receiver. The receiver structure is shown in Fig. 3.4.

As mentioned before, detecting a UWB signal coherently is a matter of matching the

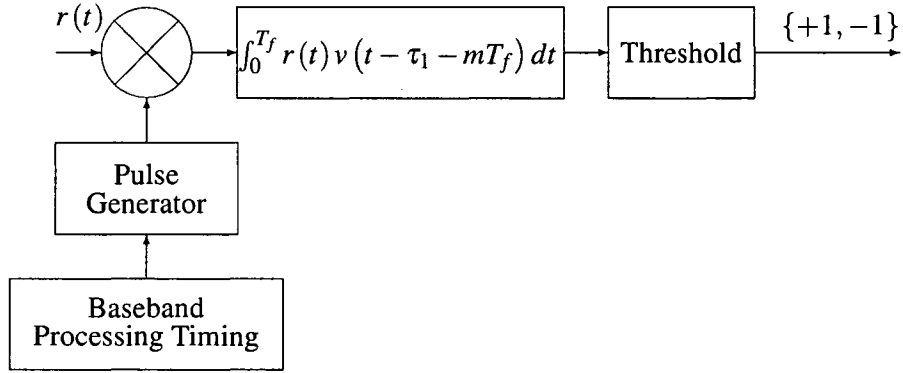


Fig. 3.4. The block diagram of the conventional matched filter UWB receiver.

received energy to a predetermined template, and the coherent detection is a mathematical operation measuring the similarity between two signals. Note that in TH-PPM systems, the information bit 0 is represented by an unaltered pulse $p(t)$, and the corresponding pulse for bit +1 is the pulse shifted by δ , $p(t - \delta)$. So, the correlation template is

$$v(t) = p(t) - p(t - \delta). \quad (3.4)$$

If the information bit +1 is sent, the received signal should have more similarity with the pulse $p(t - \delta)$ with the absence of MAI and AWGN in the channel; thus in this case, the former part of the correlator output r originating from the similarity with the pulse $p(t)$ should be smaller than the latter part originating from the similarity with $p(t - \delta)$ if the channel is not too distorting. Therefore, the correlator output, which is also referred to as the final decision statistic, is more likely to be smaller than 0 when the information bit +1 is sent, and larger than 0 when the information bit 0 is sent.

Denoting the autocorrelation function of the UWB pulse waveform $p(t)$ by $R(x)$, then another function $\tilde{R}(\Delta t)$ is defined as

$$\tilde{R}(\Delta t) = \int_{-\infty}^{\infty} p(t - \Delta t) v(t) dt \quad (3.5)$$

$$= R(\Delta t) - R(\Delta t - \delta). \quad (3.6)$$

The signal from the first user is assumed to be the desired signal and $d_0^{(1)}$ is the transmitted symbol. At the receiver side, the conventional single-user matched filter, which adopts $v(t)$ as the correlation waveform, is used to coherently detect the signal to be recovered. The correlator output is

$$r = \sum_{m=0}^{N_s-1} \int_{mT_f}^{(m+1)T_f} r(t) v(t - mT_f) dt \quad (3.7)$$

$$= S_{\text{PPM}} + I_{\text{PPM}} + N_{\text{PPM}} \quad (3.8)$$

where S_{PPM} is the desired signal term in the correlator output, which equals $A_1 \sqrt{E_b N_s} \tilde{R}(0)$ when the information bit 0 is sent, and $-A_1 \sqrt{E_b N_s} \tilde{R}(0)$ when the information bit 1 is sent. The RV N_{PPM} is Gaussian distributed with zero mean and variance $\sigma_n^2 = N_0 N_s \tilde{R}(0)$. The parameter I_{PPM} , which represents the total MAI originating from all N_s frames, can be written as

$$I_{\text{PPM}} = \frac{E_b}{N_s} \sum_{k=2}^{N_k} A_k I_{\text{PPM}}^{(k)} \quad (3.9)$$

where $I_{\text{PPM}}^{(k)}$ is the interference from the k th user and can be expressed as

$$I_{\text{PPM}}^{(k)} = \sum_{m=0}^{N_s-1} \sum_{j=-\infty}^{+\infty} \tilde{R} \left(c_j^{(k)} T_c + \delta d_{\lfloor j/N_s \rfloor}^{(k)} + \tau_k - (m - j) T_f \right). \quad (3.10)$$

We make the following assumptions:

- $N_h T_c < T_f/2 - 2T_p$, which means that the pulse can only hop over an interval of one-half of a frame time.
- τ_k is uniformly distributed on $[0, N_s T_f)$ [27].
- The chip sequences and the data information bits are independent.

The first assumption above implies that only 2 adjacent bits of the k th user, $d_{-1}^{(k)}$ and $d_0^{(k)}$ can interfere with the transmitted information bit $d_0^{(1)}$ of the desired user. Recall the partition theorem (the theorem of total probability). If the sets B_1, B_2, \dots, B_k form a partition Ω , which means they are mutually exclusive and their union $\cup_{i=1}^k B_k$ is the entire sample space Ω , i.e. one and only one of these k events will occur, the probability of an event A can be represented as

$$P(A) = \sum_{i=1}^k P(A|B_i)P(B_i). \quad (3.11)$$

Using the theorem of total probability, the characteristic function (CF) can be expanded and expressed as

$$\Phi_A(\omega) = \sum_{i=1}^k \Phi(A|B_i)P(B_i). \quad (3.12)$$

Since only 2 adjacent bits of the k th user, $d_{-1}^{(k)}$ and $d_0^{(k)}$, can interfere with the transmitted information bit $d_0^{(1)}$ of the desired user, the interference originating from $d_{-1}^{(k)}$ and $d_0^{(k)}$ form a partition of the total interference. Thus, conditioning on the delay of the k th user τ , the CF of the multiple access interference can be expressed as [19]

$$\Phi_{I_{\text{PPM}}^{(k)}|\tau}(\omega) = \Phi_{X|\tau}(\omega) \Phi_{Y|\tau}(\omega) \quad (3.13)$$

where X denotes the interference component coming from the information bit $d_{-1}^{(k)}$ and Y denotes the interference coming from the information bit $d_0^{(k)}$.

Conditioning on the delay of the k th user and the information bit $d_{-1}^{(k)}$, the conditional characteristic function, $\Phi_{X|d,\tau}(w)$, of the interference X , can be derived as [19]

$$\Phi_{X|d,\tau}(w) = \frac{1}{N_h^{N_s}} \prod_{l=1}^{N_s} \left[\sum_{h=0}^{N_h-1} \prod_{j=l}^{N_s} e^{j\omega\tilde{R}(hT_c + \delta d + \tau - jT_f)} \right]. \quad (3.14)$$

In similar fashion, conditioning on the delay of the k th user and the information bit $d_0^{(k)}$, the conditional characteristic function, $\Phi_{Y|d,\tau}(w)$, of the interference originating from $d_0^{(k)}$, can be derived as

$$\Phi_{Y|d,\tau}(w) = \frac{1}{N_h^{N_s}} \prod_{l=0}^{N_s-1} \left[\sum_{h=0}^{N_h-1} \prod_{j=0}^{N_s-l-1} e^{j\omega\tilde{R}(hT_c + \delta d + \tau - jT_f)} \right] \quad (3.15)$$

Using the partition theorem for the characteristic function, eq. (3.12), again, $\Phi_{X|\tau}(w)$ and $\Phi_{Y|\tau}(w)$ can be expressed as

$$\Phi_{X|\tau}(w) = \Phi_{X|d=0,\tau}(w) Pr(d=0) + \Phi_{X|d=1,\tau}(w) Pr(d=1) \quad (3.16)$$

and

$$\Phi_{Y|\tau}(w) = \Phi_{Y|d=0,\tau}(w) Pr(d=0) + \Phi_{Y|d=1,\tau}(w) Pr(d=1) \quad (3.17)$$

respectively. Putting (3.16) and (3.17) back into (3.13), the conditional characteristic function $\Phi_{I_{\text{PPM}}^{(k)}|\tau}(w)$ can be obtained.

Averaging (3.13) over τ , the CF of the total multiple access interference can be expressed as

$$\Phi_{I_{\text{PPM}}^{(k)}}(w) = \frac{1}{N_s T_f} \int_0^{N_s T_f} \Phi_{I_{\text{PPM}}^{(k)}|\tau}(w) d\tau \quad (3.18)$$

where τ is assumed to be uniformly distributed over $[0, N_s T_f)$.

Because of the independence of the interference from different users and the characteristics of the CF, the CF of the total interference originating from all the interferers can be represented as

$$\Phi_{I_{\text{PPM}}}(\omega) = \prod_{k=2}^{N_u} \Phi_{I_{\text{PPM}}^{(k)}} \left(A_k \sqrt{\frac{E_b}{N_s}} \omega \right). \quad (3.19)$$

The same procedure can be followed to get the CF of the total interference in TH-BPSK systems. In TH-BPSK systems, the correlation template is $p(t)$ because the information bit +1 is represented by an unaltered pulse, $p(t)$, and -1 is represented by the inverted pulse, $-p(t)$. Similar to the case for TH-PPM, the signal from the first user is assumed to be the desired signal and $d_0^{(1)}$ is the transmitted symbol. At the receiver side, the conventional single-user matched filter, which adopts $p(t)$ as the correlation waveform, is used to coherently detect the signal to be recovered. The correlator output is

$$r = \sum_{m=0}^{N_s-1} \int_{mT_f}^{(m+1)T_f} r(t) p(t - mT_f) dt \quad (3.20)$$

$$= S_{\text{BPSK}} + I_{\text{BPSK}} + N_{\text{BPSK}} \quad (3.21)$$

where $S_{\text{BPSK}} = A_1 \sqrt{E_b N_s} d_0^{(1)}$ is the desired signal term in the correlator output, which depends on the desired information bit sent by user 1. The RV N is Gaussian distributed with zero mean and variance $\sigma_n^2 = N_0 N_s / 2$. The parameter I , which represents the total MAI originating from all N_s frames, can be written as

$$I_{\text{BPSK}} = \frac{E_b}{N_s} \sum_{k=2}^{N_u} A_k I_{\text{BPSK}}^{(k)} \quad (3.22)$$

where $I^{(k)}$ is the interference from the k th user and can be expressed as

$$I_{\text{BPSK}}^{(k)} = \sum_{m=0}^{N_s-1} \sum_{j=-\infty}^{+\infty} d_{\lfloor j/N_s \rfloor}^{(k)} R\left(c_j^{(k)} T_c + \tau_k - (m-j) T_f\right) \quad (3.23)$$

We adopt the same assumption as in TH-PPM systems

- $N_h T_c < T_f/2 - 2T_p$, which means that the pulse can only hop over an interval of one-half of a frame time.
- τ_k is uniformly distributed on $[0, N_s T_f)$ as in [27].
- The chip sequences and the data information bits are independent.

The first assumption above implies that only 2 adjacent bits of the k th user, $d_{-1}^{(k)}$ and $d_0^{(k)}$ can interfere with the transmitted information bit $d_0^{(1)}$ of the desired user. Since only 2 adjacent bits can interfere with the transmitted information bit $d_0^{(1)}$, the interference originating from $d_{-1}^{(k)}$ and $d_0^{(k)}$ form a partition of the total interference. Denoting the interference from $d_{-1}^{(k)}$ by X and the interference from $d_0^{(k)}$ by Y, and conditioning on the delay of the k th user τ , the final form of the CF of the multiple access interference can be expressed as

$$\Phi_{I_{\text{BPSK}}^{(k)}|\tau}(\omega) = \Phi_{X|\tau}(\omega) \Phi_{Y|\tau}(\omega) \quad (3.24)$$

where $\Phi_{X|\tau}(\omega)$ and $\Phi_{Y|\tau}(\omega)$ are the characteristic function of the interference X and Y conditioned on the delay τ of the k th user, respectively.

If the probabilities of sending the information bit +1 and -1 are known, the partition theorem can be used again. The two conditional characteristic functions $\Phi_{X|\tau}(\omega)$ and

$\Phi_{Y|\tau}(\omega)$ can be further written as

$$\Phi_{X|\tau}(\omega) = \Phi_{X|d=-1,\tau}(\omega) Pr(d = -1) + \Phi_{X|d=+1,\tau}(\omega) Pr(d = +1) \quad (3.25)$$

and

$$\Phi_{Y|\tau}(\omega) = \Phi_{Y|d=+1,\tau}(\omega) Pr(d = +1) + \Phi_{Y|d=-1,\tau}(\omega) Pr(d = -1) \quad (3.26)$$

respectively, where $\Phi_{X|d,\tau}(\omega)$ and $\Phi_{Y|d,\tau}(\omega)$ can be represented as [19]

$$\Phi_{X|d,\tau}(\omega) = \frac{1}{N_h^{N_s}} \prod_{l=1}^{N_s} \left[\sum_{h=0}^{N_h-1} \prod_{j=l}^{N_s} e^{j\omega R(hT_c + \tau - jT_f)} \right]. \quad (3.27)$$

and

$$\Phi_{Y|d,\tau}(\omega) = \frac{1}{N_h^{N_s}} \prod_{l=0}^{N_s-1} \left[\sum_{h=0}^{N_h-1} \prod_{j=0}^{N_s-l-1} e^{j\omega dR(hT_c + \tau - jT_f)} \right]. \quad (3.28)$$

Putting (3.25) and (3.26) back to (3.24), the conditional CF of the total interference can be obtained. Averaging (3.24) over τ , the CF of the total multiple access interference can be expressed as

$$\Phi_{I_{\text{BPSK}}^{(k)}}(\omega) = \frac{1}{N_s T_f} \int_0^{N_s T_f} \Phi_{I_{\text{BPSK}}^{(k)}|\tau}(w) d\tau \quad (3.29)$$

where τ is assumed to be uniformly distributed over $[0, N_s T_f)$.

Because of the independence of the interference from different users and the characteristics of the CF, the CF of the total interference originating from all the interferers can be represented as

$$\Phi_{I_{\text{BPSK}}}(\omega) = \prod_{k=2}^{N_u} \Phi_{I_{\text{BPSK}}^{(k)}} \left(A_k \sqrt{\frac{E_b}{N_s}} \omega \right). \quad (3.30)$$

If the conventional matched filter UWB receiver is adopted to detect the signal to be recovered in the UWB systems, the decision rules of the coherent correlator output for

TH-PPM and TH-BPSK systems should be expressed as

$$\tilde{r} > 0 \Rightarrow d_0^{(1)} = 0 \quad (3.31a)$$

$$\tilde{r} \leq 0 \Rightarrow d_0^{(1)} = +1. \quad (3.31b)$$

and

$$\tilde{r} > 0 \Rightarrow d_0^{(1)} = +1 \quad (3.32a)$$

$$\tilde{r} \leq 0 \Rightarrow d_0^{(1)} = -1. \quad (3.32b)$$

respectively. Thus, the average probability of error for TH-PPM systems is

$$P_e = Pr\left(r \leq 0 | d_0^{(1)} = 0\right) \quad (3.33)$$

while the decision error for TH-BPSK systems is

$$P_e = Pr\left(r \leq 0 | d_0^{(1)} = 1\right). \quad (3.34)$$

Since the characteristic function of multiple access interference in TH-PPM and TH-BPSK systems have already been obtained, the exact BER performance of these systems can be derived using the relationship between the CDF and the CF of a RV. The relationship between the CF and CDF can be expressed as [29]

$$F_Y(y) = \frac{1}{2} + \frac{1}{\pi} \int_0^\infty \frac{\sin(y\omega)}{\omega} \Phi_Y(\omega) d\omega. \quad (3.35)$$

Thus, once the CF of the total disturbance is obtained, the bit error rate can be derived.

Denote the total disturbance by Y , and Y can be expressed as

$$Y = I_{\text{PPM}} + N_{\text{PPM}}. \quad (3.36)$$

Since the multiple access interference and background noise are independent, the CF of the total disturbance (MAI-plus-AWGN) can be written as

$$\Phi_Y(\omega) = \Phi_I(\omega) \cdot \Phi_N(\omega). \quad (3.37)$$

The bit error rate based on the decision rule for TH-PPM systems can be expressed as

$$\begin{aligned} P_{e\text{PPM}} &= Pr(r \leq 0) \\ &= Pr(S_{\text{PPM}} + I_{\text{PPM}} + N_{\text{PPM}} \leq 0) \\ &= Pr\left(A_1 \sqrt{E_b N_s} \tilde{R}(0) + I_{\text{PPM}} + N_{\text{PPM}} \leq 0\right) \\ &= Pr\left(I_{\text{PPM}} + N_{\text{PPM}} \leq -A_1 \sqrt{E_b N_s} \tilde{R}(0)\right) \\ &= 1 - F_Y\left(A_1 \sqrt{E_b N_s} \tilde{R}(0)\right). \end{aligned} \quad (3.38)$$

Use the relationship between the CF and CDF, the bit error rate can be rewritten as

$$\begin{aligned} P_{e\text{PPM}} &= \frac{1}{2} - \frac{1}{\pi} \int_0^\infty \frac{\sin A_1 \sqrt{E_b N_s} \tilde{R}(0) \omega}{\omega} \Phi_Y(\omega) d\omega \\ &= \frac{1}{2} - \frac{1}{\pi} \int_0^\infty \frac{\sin A_1 \sqrt{E_b N_s} \tilde{R}(0) \omega}{\omega} \Phi_I(\omega) \exp\left(\frac{-\sigma_n^2 \omega^2}{2}\right) d\omega. \end{aligned} \quad (3.39)$$

In similar fashion, the bit error rate can be represented by the CF of the total disturbance in the following way

$$P_{e\text{BPSK}} = \frac{1}{2} - \frac{1}{\pi} \int_0^\infty \frac{\sin(A_1 \sqrt{E_b N_s} \omega)}{\omega} \Phi_{I_{\text{BPSK}}}(\omega) \exp\left(\frac{-\sigma_{n\text{BPSK}}^2 \omega^2}{2}\right) d\omega \quad (3.40)$$

for the TH-BPSK systems.

Since the analytical expression of the average bit error rate has been obtained based on the characteristic function of multiple access interference in [19], the BER performances

of UWB systems and the validity of the Gaussian approximation can be evaluated. In [19], the CF shown above was used to get the theoretical BER of the UWB systems, and the Gaussian approximation of the total disturbance was adopted and the validity of GA was evaluated. The numerical results in [19] showed that the BER of the UWB systems computed using the exact analysis and the simulated BER are in excellent agreement with each other for all the SNR values, which confirms the accuracy of the theoretical analysis of the BER performance of the UWB systems. On the other hand, the Gaussian approximation fails to predict the error rate floor of the UWB systems. The Gaussian approximation was shown only in good agreement with the exact analysis for small SNR values. The failure of the Gaussian approximation could be explained as follows. When the SNR is small, the AWGN is the dominant term in the total disturbance, so the disturbance can be well described by a Gaussian distributed RV. On the other hand, when the value of SNR get larger and the noise term becomes smaller and no longer dominates the MAI term in the total disturbance, the disturbance cannot be well predicted by the Gaussian RV since the dominant term in this case, the multiple access interference, is not Gaussian distributed. Therefore, the Gaussian approximation is not a reliable method for predicting the BER performances for UWB systems. Actually, the Gaussian approximation underestimates the bit error rate for medium and large values of SNR and can underestimate or overestimate the improvement obtained using a longer repetition code as shown in [19]. In [19], DS-BPSK systems are also considered and some other interesting results which confirmed the invalidity of the Gaussian approximation of the total disturbance in UWB systems have

also been shown. The results reported in [30] shown that the TH-BPSK achieves the same multi-user performance as the DS-BPSK systems according to predictions obtained using the Gaussian approximation, while the actual performance of DS-BPSK systems is better than that of TH-BPSK systems for medium and large values of SNR.

Other literatures concerning the multiple access interference in UWB systems also showed that the Gaussian approximation is not so reliable to predict the performance of the UWB systems. Durisi and Romano [14] considered the TH-PPM UWB systems in their work, the additional time shift utilized by binary pulse position modulation was optimized to get the BER performance of the TH-PPM systems. The overall disturbance in this work was assumed to be a zero mean Gaussian random process. Under the hypothesis and decision rule based on this assumption, the BER performance of the TH-PPM systems was obtained and compared with the simulation results. The simulation results showed the invalidity and the extremely limited capacity for the Gaussian approximation to describe the real performance of TH-PPM technique, especially when the frame duration is much larger than the pulse duration.

3.2.2 Evaluation Based on GQR

Another useful method for evaluation of the bit error rate probability of a TH-BPSK UWB systems was proposed in [15]. This method is based on Gaussian quadrature rules, which has been widely employed for the performance evaluation of multilevel digital signals with intersymbol interference [7], and of noncoherent receivers in optimal communications [8].

The cumbersome problem of analyzing mathematically the exact pdf of MAI in UWB systems can be overcome by using this method, since only estimation of the moments of the MAI is required. It is shown in [15] that this scheme can predict the BER performance of UWB systems with satisfactory accuracy and limited computational complexity.

If TH-PPM systems is considered and the same general mathematical signal model as mentioned above is adopted, the signal can be expressed as eq. (3.1)

$$s_{\text{PPM}}^{(k)}(t) = \sqrt{\frac{E_b}{N_s}} \sum_{j=-\infty}^{+\infty} p\left(t - jT_f - c_j^{(k)}T_c - d_{\lfloor j/N_s \rfloor}^{(k)}\delta\right).$$

The receiver is also assumed to be a single-user correlator that adopts $v(t) = p(t) - p(t - \delta)$ as the correlation template. Thus, the correlator output is the same as eq. (3.9)

$$r = S_{\text{PPM}} + I_{\text{PPM}} + N_{\text{PPM}}$$

where S_{PPM} is the desired signal term in the correlator output and I_{PPM} represents the total MAI originating from all N_s frames. The RV N_{PPM} is Gaussian distributed with zero mean and variance $\sigma_n^2 = N_0 N_s \tilde{R}(0)$.

Assume that the MAI term is known, and the average bit error rate P_e can be expressed in terms of the conditional probability as

$$P_e = E_{\text{MAI}} \left[\frac{1}{2} \text{erfc} \left(\frac{S_{\text{PPM}} + I_{\text{PPM}}}{\sqrt{2}\sigma_n} \right) \right]. \quad (3.41)$$

Since mathematically analyzing the pdf of MAI was proved to be a cumbersome problem, it is not tractable to evaluate eq. (3.41) based on the true pdf of the interference term. A practical method based on GQR can be introduced [15]. According to the GQR technique,

an integral containing a certain pdf can be represented as

$$\int_a^b g(x) f_X(x) dx = \sum_{i=1}^N w_i g(x_i) + E_N \quad (3.42)$$

where $\{x_i\}_{i=1}^N$ and $\{w_i\}_{i=1}^N$ are the abscissas and the weights obtained by the GQR rule, and their values depend on the integration interval and the form of the pdf. The parameter E_N is the truncation error. Adopting the algorithm in [20], only the first $2N-1$ moments of the RV X need be known to calculate eq. (3.42). Following the same procedure in [15] and adopting the assumption that the delays $\{\tau_k\}_{k=2}^{N_u}$ are uniformly distributed on the bit transmission duration, the moments of the RV MAI can be obtained with the aid of the technique described in [21], and the BER performance can be evaluated using eq. (3.41) and eq. (3.42). The method's accuracy was confirmed by simulation results since the BER curves obtained by GQR perfectly agree with simulated curves. Subsequently, the actual BER performances were compared with the results obtained based on Gaussian approximations. It was shown that Gaussian approximations highly underestimate the BER of TH-PPM systems for medium and large values of SNR, which confirms the invalidity of the Gaussian approximation for the MAI in UWB systems.

3.3 Other Approximations of the Multiple Access Interference and New Receiver Designs

Since the Gaussian approximation is invalid and not suitable to describe the BER performance of UWB systems and the conventional matched filter UWB receiver, which was

widely adopted in the UWB systems, is not necessarily the optimal receiver, studies concerning the statistics of the multiple access interference are still going on, and the search for the optimal receiver or at least a better receiver for UWB systems continues.

Note that the short bursts of multiple access interference are impulse-like, and the Laplace noise model is used for impulsive noise. Therefore, the adoption of the Laplacian approximation for the multiple access interference in UWB systems becomes reasonable.

Schwartz and Shaw [22] gave a good exposition of the problem of detecting the presence or absence of a signal embedded in Laplacian noise. We will repeat this theory here and then describe how it was adopted in [24] and [25] to the data communication problem.

Recall the Neyman-Pearson optimal detector for detecting the presence or absence of an additive signal in independent Laplacian noise in [23]. The pdf of the Laplace noise model is given by

$$f(x) = \frac{\gamma}{2} e^{-\gamma|x-\mu|}. \quad (3.43)$$

For a Laplacian distributed RV, the mean and variance are $E(x) = \mu$ and $var(x) = 2/\gamma^2$, respectively. Consider the hypothesis test

$$H_0: Y_i = N_i, \quad i = 1, 2, \dots, n$$

$$H_1: Y_i = N_i + S_i$$

where n is the number of samples, the RVs $\{N_i\}_{i=1}^n$ are independent samples of Laplacian distributed noise and the $\{S_i\}_{i=1}^n$ are samples of the additive signal. That is, H_0 is the hypothesis that only noise is present, and H_1 is the hypothesis that signal plus noise

is present. Some notations and terminology are used here as in [23]. Let α denote the false alarm probability which is defined as the probability of announcing H_1 while H_0 was true, and the detection probability β is defined as the detection probability, which is the probability of announcing H_1 when H_1 is true. A detector is said to be optimal in the Neyman-Pearson sense if the detection probability β is maximized subject to a constraint on the false alarm probability. The final partial decision statistics are obtained from the single sample log-likelihood ratio $\log L_i(y)$ given by

$$g_i(y) = \log L_i(y) = \log \left(\frac{e^{-\gamma|y-S_i|}}{e^{-\gamma|y|}} \right). \quad (3.44)$$

The partial decision statistics $g_i(y)$ can be simplified as

$$g_i(y) = \begin{cases} -\gamma S_i & y < 0 \\ 2\gamma y - \gamma S_i & 0 \leq y \leq S_i \\ \gamma S_i & y > S_i \end{cases} \quad (3.45)$$

and the final decision statistic can be expressed as

$$T = \sum_{i=1}^n g_i(y_i) \quad (3.46)$$

where the sequence of RVs $\{y_i\}_{i=1}^n$ represents the data samples. The optimal test compares T to a prescribed threshold T_s and declares H_0 if the final statistic $T < T_s$ and declares H_1 if $T > T_s$. If $T = T_s$, the optimal test declares H_0 with probability q and H_1 with probability p , where $p + q = 1$.

Beaulieu and Hu [24] introduced the optimal receiver for the signals corrupted by Laplacian noise in UWB systems for the first time by adopting the signal detection model

and analysis in [22] to the binary data communication problem. The proposal to use it in UWB systems was new and motivated by the impulse-like multiple access interference in the systems. TH-BPSK UWB systems was considered. The decision statistic of the conventional single-user correlation receiver was obtained in this work as

$$\begin{aligned} r &= \sum_{m=0}^{N_s-1} \int_{mT_f}^{(m+1)T_f} r(t) p(t - \tau_1 - mT_f) \\ &= S + I \end{aligned} \quad (3.47)$$

where the notations are the same as defined before. The assumptions that the delays $\{\tau_k\}_{k=2}^{N_s}$ are uniformly distributed in the region $[0, N_s T_f]$ is adopted, and the condition $N_h T_c < \frac{T_f}{2} - 2T_p$, which means that the pulse can only hop over an interval of one-half of a frame time, is also assumed. Then the final statistic r can be rewritten as [24]

$$\begin{aligned} r &= \sum_{m=0}^{N_s-1} r_m \\ &= \sum_{m=0}^{N_s-1} S_m + I_m \end{aligned} \quad (3.48)$$

where r_m is the correlator output of a single frame which is the sum of S_m and I_m , which are the desired signal component and the total interference component in the m th frame, respectively. The interference term I_m can be further expressed as

$$I_m = \sqrt{\frac{E_b}{N_s}} \sum_{k=2}^{N_u} A_k d_{[(m+m_k)/N_s]}^{(k)} R(\alpha_k + c_m^{(k)} T_c). \quad (3.49)$$

Assuming that the interference $\{I_m\}_{m=0}^{N_s-1}$ are independent from each other, and that the multiple access interference in each frame can be modeled as Laplacian distributed, the optimal receiver proposed in [23] can be introduced to detect TH-BPSK signals [24]. The

final decision statistic of this new receiver is different from the conventional matched filter UWB receiver, which makes its decision based on $r = \sum_{m=0}^{N_s-1} r_m$. Its decision statistic was obtained as

$$\tilde{r} = \sum_{m=0}^{N_s-1} \tilde{r}_m \quad (3.50)$$

where \tilde{r}_m is the optimal detector nonlinearity obtained from the single sample log-likelihood ratio and can be written as

$$\tilde{r}_m = \begin{cases} |S_m| & |S_m| \leq r_m \\ r_m & -|S_m| \leq r_m \leq |S_m| \\ -|S_m| & r_m \leq -|S_m|. \end{cases} \quad (3.51)$$

The simulation results in [24] showed that the new receiver, dubbed the soft-limiting UWB receiver, can achieve large gains in the absence of AWGN. In more practical environments where both MAI and AWGN are present, it underperforms the conventional matched filter UWB receiver for small SNR values. However, its BER performance surpasses that of the conventional matched filter UWB receiver for medium and large values of SNR.

Note that if the limiter thresholds are set to infinity, the soft-limiting receiver is the same as the conventional matched filter. Thus, if the threshold of the soft-limiting receiver is adaptive, the resultant receiver structure should always performs at least as well as the conventional matched filter UWB receiver at arbitrary values of SIR and SNR. A new receiver design based on these observations was proposed in [25]. The simulation results in this work showed that the new receiver, dubbed the adaptive threshold soft-limiting UWB receiver, can always achieve better performance than the conventional matched filter UWB

receiver.

3.4 Summary

In this chapter, the framework and the general mathematical expressions of time-hopping UWB systems were introduced. Then the previous work on the BER performance of UWB systems were briefly recalled, including the method of evaluating the BER performance of UWB systems using the characteristic functions of the MAI proposed in [19], and the one using GQR proposed in [15]. These work all showed that the Gaussian approximation for the MAI is not valid to predict the BER performance of UWB systems. Thus, other approximations and the corresponding receiver design proposed recently were also discussed in this chapter. The recently proposed UWB receivers were shown to have better performance than the conventional matched filter UWB receiver although they are still the suboptimal receiver for UWB systems.

Chapter 4

Novel Zonal UWB Receiver

It was explained in previous chapters that the multiple access interference of UWB systems cannot be well approximated by a Gaussian distributed RV, and Gaussian approximations can highly underestimate the BER performance of UWB systems. The studies concerning the statistics of the multiple access interference continue and researchers want to find the exact pdf of the MAI based on which an optimal receiver design can be derived. However, it has been shown that evaluating the exact pdf of the MAI is cumbersome. Thus, other distributions are introduced to approximate the pdf of the MAI in UWB systems. For example, the Laplacian approximation for the MAI was proposed based on the observations that the short bursts of multiuser interference in UWB systems are impulse-like. The optimal receiver structure based on the Laplacian approximation has been introduced in UWB systems. The newly proposed UWB receiver was shown to have better BER performance than the conventional matched filter UWB receiver in pure MAI channels. This fact implies

that the Laplacian approximation works better than the Gaussian distribution for predicting the BER performance of UWB systems. However, the adoption of the Laplacian approximation and the introduction of the corresponding UWB receiver were ad hoc intuitive choices since there was no evidence showing that the MAI in UWB systems is Laplacian distributed. Hence, there is no reason to believe that the optimal Laplacian receiver is the optimal UWB receiver in the minimum probability of error sense for the MAI alone, or for a mixture of MAI and AWGN. Although it is not tractable to derive rigorously an optimal receiver design using ML receiver design principles based on the exact pdf of the MAI, a better UWB receiver can still be designed based on the observations of the simulated pdf of the MAI in UWB systems.

A novel UWB receiver structure dubbed the “zonal” receiver is proposed in this way to detect TH-UWB signals in MAI channels. The zonal receiver outperforms the conventional matched filter UWB receiver and the recently proposed soft-limiting UWB receiver in multiple access interference channels. In more practical multiple access interference-plus-noise environments, the zonal UWB receiver achieves better performance than the conventional matched filter UWB receiver and its bit error rate performance surpasses that of the recently proposed adaptive threshold soft-limiting UWB receiver for large values of signal-to-noise ratio.

4.1 System Models

In this development, only time-hopping binary phase-shift keying (TH-BPSK) is considered. The analysis and results are similar for a binary pulse position modulation (PPM) system. A TH-BPSK signal can be described as [19]

$$s^{(k)}(t) = \sqrt{\frac{E_b}{N_s}} \sum_{j=-\infty}^{+\infty} d_{\lfloor j/N_s \rfloor}^{(k)} p(t - jT_f - c_j^{(k)}T_c) \quad (4.1)$$

where t is the transmitter clock time, $s^{(k)}(t)$ is the signal of the k th user, and the other notations and terminologies are as follows

- $d_j^{(k)}$ is the j th information bit of the k th user, which takes values from $\{+1, -1\}$ with equal probabilities.
- The function $p(t)$ is the transmitted UWB pulse with unit energy, i.e. $\int_{-\infty}^{+\infty} p^2(t) dt = 1$.
- E_b is the bit energy, N_s is the number of frames which are used to transmit a single information bit, which is also known as the length of the repetition code. As mentioned in previous chapters, $\sqrt{E_b/N_s}$ is the normalization factor that make all the systems have the same energy in the information bit.
- T_f is the duration of a single frame. Each time frame is divided into chips with duration T_c . The relationship between T_f and T_c is $T_c N_h = T_f$, where N_h is the number of hops in each time frame.
- The sequence $\{c_j^{(k)}\}$ is the time-hopping sequence for each bit of the k th user which takes integer values in the range $0 \leq c_j^{(k)} < N_h$. The product $c_j^{(k)}T_c$ represents an additional time shift added to the TH pulses to avoid catastrophic collisions between multiple users.

Assuming ideal free-space propagation for clarity, when there are N_u transmitters in the same coverage area, the received signal can be written as

$$r(t) = \sum_{k=1}^{N_u} A_k s^{(k)}(t - \tau_k) + n(t) \quad (4.2)$$

where $n(t)$ is AWGN with two-sided power spectral density $N_0/2$, and the sequences $\{A_k\}_{k=1}^{N_u}$ and $\{\tau_k\}_{k=1}^{N_u}$ are the attenuations and delays of the k th user, respectively. The random variables (RVs) $\{\tau_k\}_{k=2}^{N_u}$ can be assumed to be uniformly distributed on $[0, T_b)$ [19], [27].

4.2 Receiver Structure

At the receiver side, we assume that the signal from the first user is the desired signal and $d_0^{(1)}$ is the transmitted symbol. Without loss of generality, $c_j^{(1)}$ is set to zero, for all j [15]. When the conventional single-user matched filter is used to coherently detect the signal to be recovered, the received decision statistic is

$$\begin{aligned} r &= \sum_{m=0}^{N_s-1} \int_{mT_f+\tau_1}^{(m+1)T_f+\tau_1} r(t) p(t - \tau_1 - mT_f) dt \\ &= \sum_{m=0}^{N_s-1} \sum_{k=1}^{N_u} \int_{mT_f+\tau_1}^{(m+1)T_f+\tau_1} A_k s(t - \tau_k) p(t - \tau_1 - mT_f) dt \\ &= S + I + N \end{aligned} \quad (4.3)$$

where N is a Gaussian RV with zero mean and variance $N_0 N_s / 2$, and $S = A_1 \sqrt{E_b N_s} d_0^{(1)}$ where $d_0^{(1)}$ is the information bit transmitted by the desired user. The parameter I is the

total MAI originating from all N_s frames, which can be represented as

$$I = \sqrt{\frac{E_b}{N_s}} \sum_{k=2}^{N_u} A_k I^{(k)} \quad (4.4)$$

where $I^{(k)}$ can be expressed as

$$I^{(k)} = \sum_{m=0}^{N_s-1} \int_{mT_f+\tau_1}^{(m+1)T_f+\tau_1} s^{(k)}(t-\tau_k) p(t-\tau_1-mT_f) dt. \quad (4.5)$$

Substituting (4.1) into (4.5) and denoting the autocorrelation function of the UWB pulse waveform $p(t)$ by $R(x)$, $I^{(k)}$ can be rewritten as

$$I^{(k)} = \sum_{m=0}^{N_s-1} \sum_{j=-\infty}^{+\infty} d_{\lfloor j/N_s \rfloor}^{(k)} R\left(\tau_1 - \tau_k + mT_f - jT_f - c_j^{(k)} T_c\right). \quad (4.6)$$

Note that there are two large time uncertainties in the argument of $R(\cdot)$, which are the transmission reference time τ_1 and τ_k . These two RVs are concerning the times when the radios begin transmission in asynchronous operation, and the uncertainty related to their difference may span an interval of length many times the frame duration T_f . The time shift difference between different users can be modeled as [3]

$$\tau_1 - \tau_k = m_k T_f + \alpha_k \quad (4.7)$$

where m_k is the value of the time uncertainty rounded to the nearest integer, and α_k is the error and fractional part in the rounding process, which is uniformly distributed in the interval $(-T_f/2, T_f/2]$. Then the argument of $R(\cdot)$ is

$$(m + m_k - j) T_f \underbrace{\overbrace{-c_j^{(k)} T_c}^{\text{magnitude} \leq N_h T_c} + \overbrace{\alpha_k}^{\text{magnitude} \leq T_f/2}}_{\text{magnitude} \leq T_f/2 + N_h T_c}. \quad (4.8)$$

We now adopt the assumption $N_h T_c < T_f/2 - 2T_p$ in [3], which means that the pulse can only hop over an interval of one-half of a frame time. Thus, the term $-c_j^{(k)} T_c + \alpha_k$ satisfies the condition that

$$-c_j^{(k)} T_c + \alpha_k \leq T_f - 2T_p. \quad (4.9)$$

Then $I^{(k)}$ can be expressed as

$$\begin{aligned} I^{(k)} &= \sum_{m=0}^{N_s-1} \sum_{j=-\infty}^{+\infty} d_{\lfloor j/N_s \rfloor}^{(k)} R\left(\tau_1 - \tau_k + mT_f - jT_f - c_j^{(k)} T_c\right) \\ &= \sum_{m=0}^{N_s-1} \sum_{j=-\infty}^{+\infty} d_{\lfloor (m+m_k)/N_s \rfloor}^{(k)} R\left((m+m_k-j)T_f \underbrace{-c_j^{(k)} T_c + \alpha_k}_{\text{magnitude} \leq T_f - 2T_p} \right) \end{aligned} \quad (4.10)$$

The waveform $p(t)$ is only nonzero in the time interval $[0, T_p]$, and the support of the autocorrelation function $R(\cdot)$ is $[-T_p, T_p]$. Since $T_p \ll T_f$, only one term in the sum of j in eq. (4.10) can be nonzero, and this nonzero term appears when the condition $j = m + m_k$ is satisfied. Thus, the interference from the k th user can be rewritten as

$$\begin{aligned} I^{(k)} &= \sum_{m=0}^{N_s-1} \sum_{j=-\infty}^{+\infty} d_{\lfloor (m+m_k)/N_s \rfloor}^{(k)} R\left((m+m_k-j)T_f - c_j^{(k)} T_c + \alpha_k \right) \\ &= \sum_{m=0}^{N_s-1} d_{\lfloor (m+m_k)/N_s \rfloor}^{(k)} R\left(\alpha_k - c_{m+m_k}^{(k)} T_c \right) \end{aligned} \quad (4.11)$$

On the other hand, if the condition (4.7) is not satisfied, then there might be more than one nonzero term in the sum of j , and the actual value should be determined by the RV involved.

Putting (4.11) back into (4.4), the total interference term can be expressed as

$$\begin{aligned}
I &= \sqrt{\frac{E_b}{N_s}} \sum_{k=2}^{N_u} A_k \sum_{m=0}^{N_s-1} d_{\lfloor (m+m_k)/N_s \rfloor}^{(k)} R\left(\alpha_k - c_{m+m_k}^{(k)} T_c\right) \\
&= \sum_{m=0}^{N_s-1} \sum_{k=2}^{N_u} \sqrt{\frac{E_b}{N_s}} A_k d_{\lfloor (m+m_k)/N_s \rfloor}^{(k)} R\left(\alpha_k - c_{m+m_k}^{(k)} T_c\right) \\
&= \sum_{m=0}^{N_s-1} I_m
\end{aligned} \tag{4.12}$$

where I_m is the interference term on each frame, which is given by

$$I_m = \sum_{k=2}^{N_u} \sqrt{\frac{E_b}{N_s}} A_k d_{\lfloor (m+m_k)/N_s \rfloor}^{(k)} R\left(\alpha_k - c_{m+m_k}^{(k)} T_c\right). \tag{4.13}$$

Then the final receiver decision statistic can be expressed as a summation of statistics in each frame

$$\begin{aligned}
r &= \sum_{m=0}^{N_s-1} r_m = \sum_{m=0}^{N_s-1} (S_m + I_m + N_m) \\
&= \sum_{m=0}^{N_s-1} (S_m + Y_m)
\end{aligned} \tag{4.14}$$

where $S_m = A_1 \sqrt{E_b/N_s} d_0^{(1)}$ is desired signal component in the m th frame, N_m is a Gaussian distributed RV with variance $N_0/2$, and I_m is the total interference component in the m th frame from all interferers given in (4.13). The RV Y_m is the overall disturbance (MAI plus AWGN) in the m th frame.

If we consider the case where the MAI dominates the AWGN, the noise term is negligible compared with the MAI component and r_m can be expressed as $I_m + S_m$. Fig. (4.1) shows an example of the form of the conditional probability density function (pdf) of the chip correlator output r_m when the information bit +1 was sent, $f\left(r_m | d_0^{(1)} = +1\right)$. These

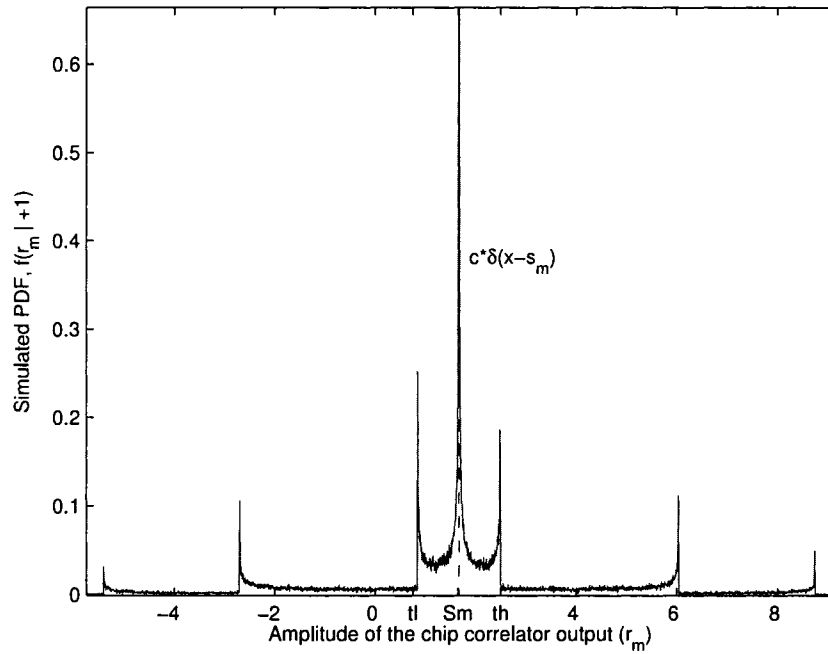


Fig. 4.1. The simulated conditional probability density function (pdf) $f(r_m | d_0^{(1)} = +1)$ of the amplitude of the chip correlator output $r_m = S_m + I_m$, where I_m is the MAI in m th frame, the SIR = 10 dB, and c is a constant.

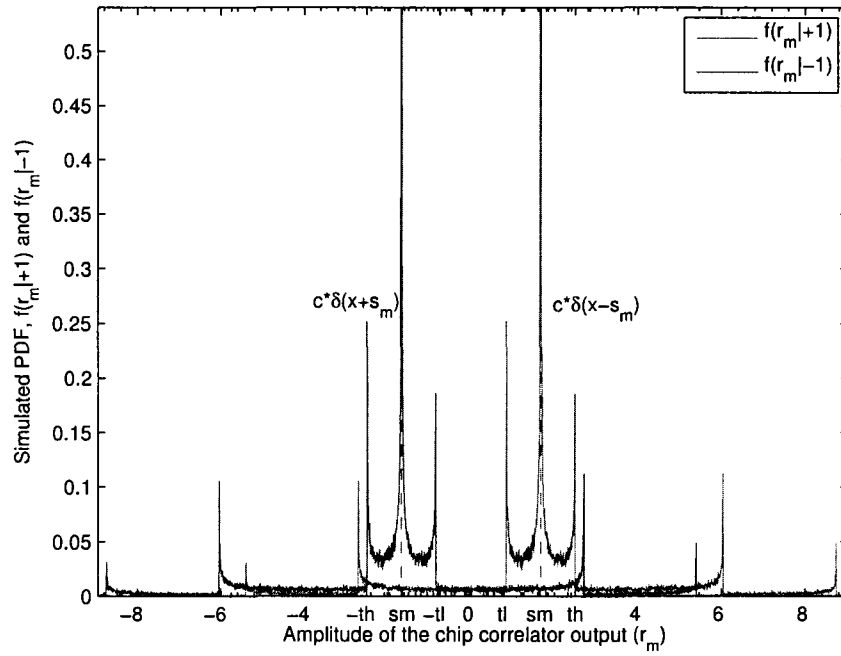


Fig. 4.2. The simulated conditional probability density functions (pdfs) $f(r_m|d_0^{(1)} = +1)$ and $f(r_m|d_0^{(1)} = -1)$ of the amplitude of the chip correlator output $r_m = S_m + I_m$, where I_m is the MAI in m th frame, the SIR = 10 dB, and c is a constant.

results are obtained by simulation. The following observations can be noted. There is an impulse at the point $r_m = S_m$ and the probability that r_m assumes values in the region (t_l, t_h) is significant, as large or larger than the probability that r_m falls outside of (t_l, t_h) , where t_l and t_h are two thresholds shown in Fig. 4.1. Fig. 4.2 shows $f(r_m|d_0^{(1)} = +1)$ and $f(r_m|d_0^{(1)} = -1)$ together, which are the pdf of the chip correlator output r_m when the information bit +1 and -1 were sent, respectively.

Recall that the optimal, minimum probability of error, decision rule operating on N_s independent samples, $\{r_m\}_{m=0}^{N_s-1}$, specifies that the receiver decides which information bit was sent according to following principles [28],

$$\prod_{m=0}^{N_s-1} f(r_m|d_0^{(1)} = +1) > \prod_{m=0}^{N_s-1} f(r_m|d_0^{(1)} = -1) \Rightarrow d_0^{(1)} = +1 \quad (4.15a)$$

$$\prod_{m=0}^{N_s-1} f(r_m|d_0^{(1)} = -1) > \prod_{m=0}^{N_s-1} f(r_m|d_0^{(1)} = +1) \Rightarrow d_0^{(1)} = -1. \quad (4.15b)$$

Observe in Fig. 4.2 that if r_m falls outside $(-t_h, -t_l)$ and (t_l, t_h) , it is unreliable to decide the transmitted information bit as +1 or -1 because $f(r_m|d_0^{(1)} = +1)$ and $f(r_m|d_0^{(1)} = -1)$ are small and almost the same outside these regions, while if r_m falls inside $(-t_h, -t_l)$, there is a relatively large probability that the transmitted information bit is -1 and if r_m falls into (t_l, t_h) , the corresponding information bit is more likely to be +1.

Based on these observations and considerations, we propose a new UWB receiver structure. Instead of making a decision based on the statistic $r = \sum_{m=0}^{N_s-1} r_m$, the new receiver will decide the transmitted signal based on a new final decision statistic \tilde{r} , which is calculated

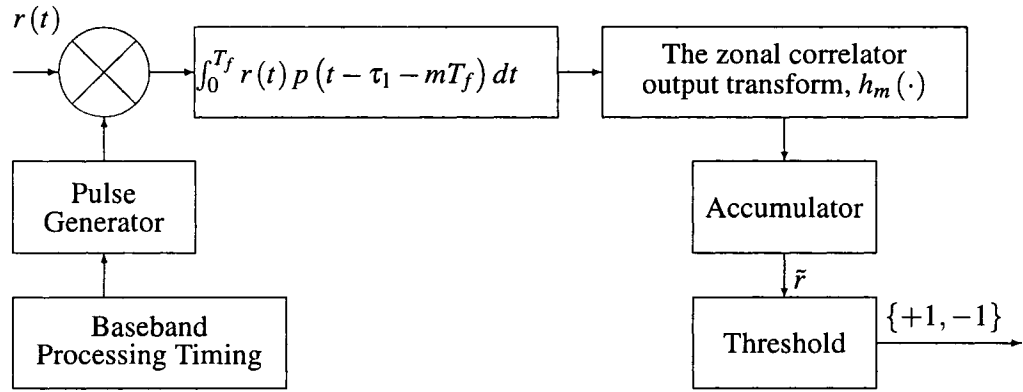


Fig. 4.3. The block diagram of the zonal UWB receiver.

as

$$\tilde{r} = \sum_{m=0}^{N_s-1} \tilde{r}_m \quad (4.16)$$

where the new partial statistics \tilde{r}_m are obtained as

$$\tilde{r}_m = \begin{cases} r_m, & r_m \in (-t_h, -t_l) \text{ or } r_m \in (t_l, t_h) \\ 0, & \text{otherwise.} \end{cases} \quad (4.17)$$

Eq. (4.17) defines a transform of the chip correlator output, r_m , into a partial receiver statistic, \tilde{r}_m . The transmitted information bit $d_0^{(1)}$ is detected based on the new decision statistic \tilde{r} according to the rule

$$\tilde{r} > 0 \Rightarrow d_0^{(1)} = +1 \quad (4.18a)$$

$$\tilde{r} < 0 \Rightarrow d_0^{(1)} = -1. \quad (4.18b)$$

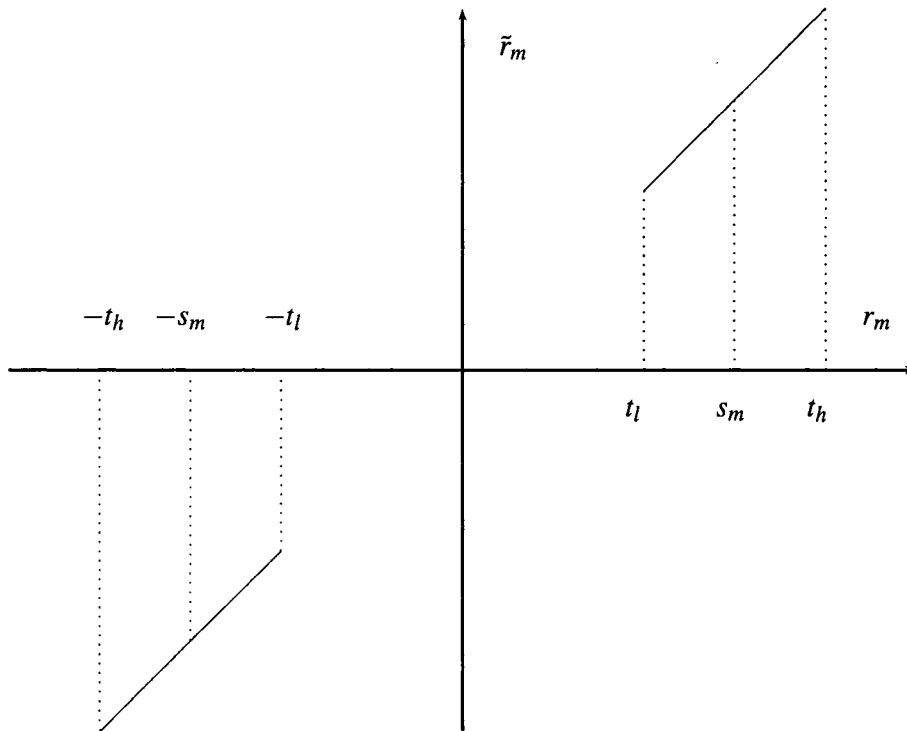


Fig. 4.4. The transfer characteristic of the receiver chip correlator output transform.

If $\tilde{r} = 0$, a fair coin is tossed to decide which information bit was transmitted. A block diagram showing the structure of the zonal UWB receiver is given in Fig. 4.3. Fig. 4.4 shows the transfer characteristic of the receiver chip correlator output transform.

The zonal receiver design rule (4.17) is intuitive. If the chip correlator output r_m falls into the region (t_l, t_h) , there is a relative large probability that the transmitted information bit is $+1$, and if r_m falls into $(-t_h, -t_l)$, the transmitted information bit is more likely to be -1 . So if the chip correlator output r_m falls into (t_l, t_h) or $(-t_h, -t_l)$, the zonal UWB receiver uses the sample unaltered and lets it contribute to the final receiver decision statistic \tilde{r} . On the other hand, if r_m falls outside of these two regions, one can hardly discern

which information bit was transmitted; in this case, the receiver discards the sample and adds 0 to \tilde{r} to eliminate r_m 's effect on the final decision statistic. Observe also that a large impulse of interference in a frame is completely eliminated from the decision statistic if it is greater than $|t_h|$ in amplitude. This feature gives the zonal receiver robustness in impulsive interference, regardless of the distribution of the impulsive interference.

We emphasize that the design of the new UWB receiver structure is based intuitively on the qualitative nature of the simulated pdf of the chip correlator output r_m . That is, the zonal UWB receiver is not necessarily optimal. The design of the optimal receiver for UWB systems requires knowledge about the exact pdf of the multiple access interference. However, characterizing mathematically the pdf in Fig. 4.1 seems difficult. Hence, it is not tractable to derive rigorously an optimal receiver design using ML receiver design principles. Observe, however, that if we set the lower threshold t_l to 0 and the upper threshold t_h to infinity, the zonal receiver becomes exactly the conventional matched filter UWB receiver. This implies that if we make the thresholds t_l and t_h adaptive, the zonal UWB receiver can always meet or outperform the conventional matched filter UWB receiver. This will be true for arbitrary additive signal disturbances, including MAI, AWGN, and MAI-plus-AWGN.

4.3 Validity of Zonal UWB Receiver Design

The simulated pdfs of the MAI in UWB systems shown in Fig. 4.1 and Fig. 4.2 are the basis of the zonal UWB receiver design. Since N_u and N_s all assume small values in the simulations, one may be concerned that in practical systems with larger values of N_u and

N_s , the central limit theorem may be applied and the MAI is thus Gaussian distributed. If this concern is true, the conventional matched filter UWB receiver should work better than the zonal UWB receiver, and then the design of the zonal UWB receiver may be less significant.

It is shown in Fig. 4.1 and Fig. 4.2 that there is an impulse at the point $r_m = S_m$ when the transmitted information bit is +1, while the impulse appears at the point $r_m = -S_m$ when the information bit -1 is sent. A simplified example used to analyze the MAI term originating from a single interferer can be used to explain the existence of the impulse. Single user detection is used at the receiver side. The duration of the UWB pulse $p(t)$ is τ_p , the frame duration is T_f , and the time shift difference between the desired signal and the interfering signal is τ . The attenuations of the desired user and the interfering user are A_0 and A_k , respectively. Thus, in this case, the received signal can be expressed as

$$r(t) = A_0 p(t) + A_k p(t - \tau) + n_0(t) \quad (4.19)$$

where $n_0(t)$ is AWGN with two-sided power spectral density $N_0/2$. Let $R(\cdot)$ denote the autocorrelation function of the UWB pulse $p(t)$. Assuming perfect synchronization of the desired user, the partial decision statistic r_m in a single frame can be obtained after the coherent correlator as

$$\begin{aligned} r_m &= \int_0^{T_f} r(t) p(t) dt \\ &= A_0 R(0) + A_k R(\tau) + \int_0^{T_f} n_0(t) g(t) dt \\ &= S_m + I_m + N_m \end{aligned} \quad (4.20)$$

where $S_m = A_0R(0)$ is the desired signal component, and $N_m = \int_0^{T_f} n_0(t)g(t)dt$ is the AWGN component. The multiple access interference term in this case, I_m , in the partial decision statistic is expressed as $I = A_kR(\tau)$, where the argument of the autocorrelation function $R(\cdot)$, τ , is a RV uniformly distributed in the region $[-\frac{T_f}{2}, \frac{T_f}{2}]$. The relationship between the time shift difference τ and the interference I_m is illustrated in Fig. 4.5.

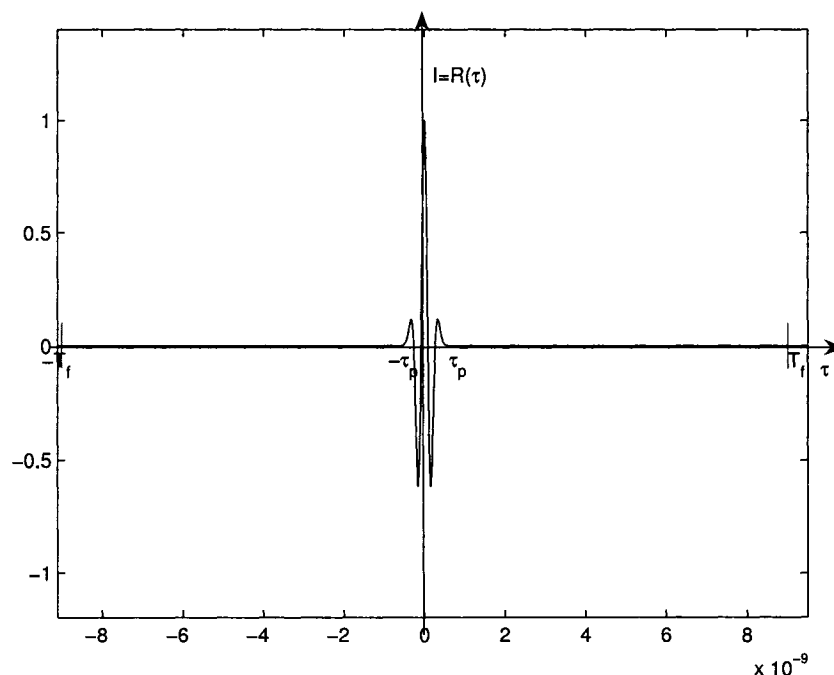


Fig. 4.5. The relationship between the time shift difference τ and the interference term I_m .

From Fig. 4.5, it is obvious that the probability that the interference assumes the value 0 is

$$\begin{aligned}
 P_r\{I_m = 0\} &= P_r\{\tau \in (-T_f/2, -\tau_p) \text{ or } \tau \in (\tau_p, T_f/2)\} \\
 &= 1 - \frac{2\tau_p}{T_f}.
 \end{aligned} \tag{4.21}$$

Since in practical UWB systems, $\tau_p \ll T_f$, there is a very large spike at the origin. The analysis for larger N_s and N_u is the same as above. The spike at the origin point makes the central limit theorem effect converge very slowly with the increase of the number of users and the length of repetition code. Furthermore, UWB is suited to enhance commercial products with wireless connectivity or to implement wireless personal area networks (WPAN), which are connected in a short range. Thus, the number of users in the same coverage area is not large enough for the central limit theorem to apply. In this case, the conventional matched filter UWB receiver is not necessarily the optimal receiver, and the design of the zonal UWB receiver is superior.

4.4 Performance Results

In this section, we evaluate the average bit error rate (BER) performance of the zonal UWB receiver and compare it to the conventional matched filter UWB receiver, the soft-limiting UWB receiver proposed in [24] and the adaptive threshold soft-limiting UWB receiver proposed in [25]. The signal waveform is restricted to the second-order Gaussian monocycle with parameters give in Table 4.1. Simulations are carried out for 2 cases. The first case is when only MAI is present in the channel, representing interference-limited operation. The second case is when both MAI and AWGN are present in the channel. In both cases, we assume perfect synchronization of the desired user, i.e., the delay of the desired user, τ_1 , is known to the receiver, and the receiver will use the information for coherent correlation.

The BER performance will be evaluated in terms of the SIR and SNR, where the SNR

TABLE 4.1

Parameters of the UWB system

Parameter	Notation	values
Time Normalization Factor	τ_p	0.2877 ns
Frame width	T_f	20 ns
Chip width	T_c	0.9 ns
No. of Users	N_u	4
No. of Chips per Frame	N_h	8
Repetition Code Length	N_s	4

is defined as

$$SNR = \frac{E_b}{N_0} \quad (4.22)$$

The variance of the total interference can be expressed as [3]

$$\begin{aligned}
 \text{var}[I] &= E[I^2] - E^2[I] \\
 &= E \left[\left(\sqrt{E_b/N_s} \sum_{k=2}^{N_u} A_k I^{(k)} \right)^2 \right] \\
 &= E_b \sigma_a^2 \sum_{k=2}^{N_u} A_k
 \end{aligned} \quad (4.23)$$

where σ_a^2 is defined as [3]

$$\begin{aligned}
 \sigma_a^2 &= \frac{1}{T_f} \int_{-\infty}^{+\infty} \left[\int_{-\infty}^{+\infty} p(x-t) p(x) dx \right]^2 dt \\
 &= \frac{1}{T_f} \int_{-\infty}^{+\infty} R^2(t) dt
 \end{aligned} \quad (4.24)$$

where $R(t)$ is the autocorrelation function of the second-order Gaussian monocycle. Thus, it is reasonable to define the SIR as

$$\begin{aligned} SIR &= \frac{A_1^2 E_b N_s}{\text{var}[I]} \\ &= \frac{A_1^2 N_s}{\sigma_a^2 \sum_{k=2}^{N_u} A_k^2}. \end{aligned} \quad (4.25)$$

4.4.1 Performance in pure MAI channels

We evaluate the BER performance of the zonal UWB receiver in channels where only MAI is present, and compare it to those of the conventional matched filter UWB receiver and the recently proposed soft-limiting UWB receiver. Monte-Carlo simulation is used for estimating the BER, and as mentioned above, the waveform used in TH-BPSK systems is restricted to the second-order Gaussian monocycle and the parameters are as in Table 4.1.

First, BER performances of the TH-BPSK systems with 3 interferers are plotted versus SIR. Fig. 4.6 shows the BER curves for the conventional matched filter UWB receiver, the soft-limiting UWB receiver and the zonal UWB receiver with fixed thresholds when only MAI is present in the channel, and $S_m - 0.05$ and $S_m + 0.05$ are adopted as the lower and upper thresholds. Observe that in the SIR region [-8 dB, 14 dB], the zonal UWB receiver with fixed thresholds outperforms the other two UWB receivers. The performance gains are significant when the SIR is small. The BER of the zonal UWB receiver is as much as 50 times smaller than the BER of the conventional matched filter UWB receiver, and as much as 10 times smaller than the BER of the soft-limiting receiver in this SIR region. We hasten to point out that these large gains can not be achieved when there is AWGN in the

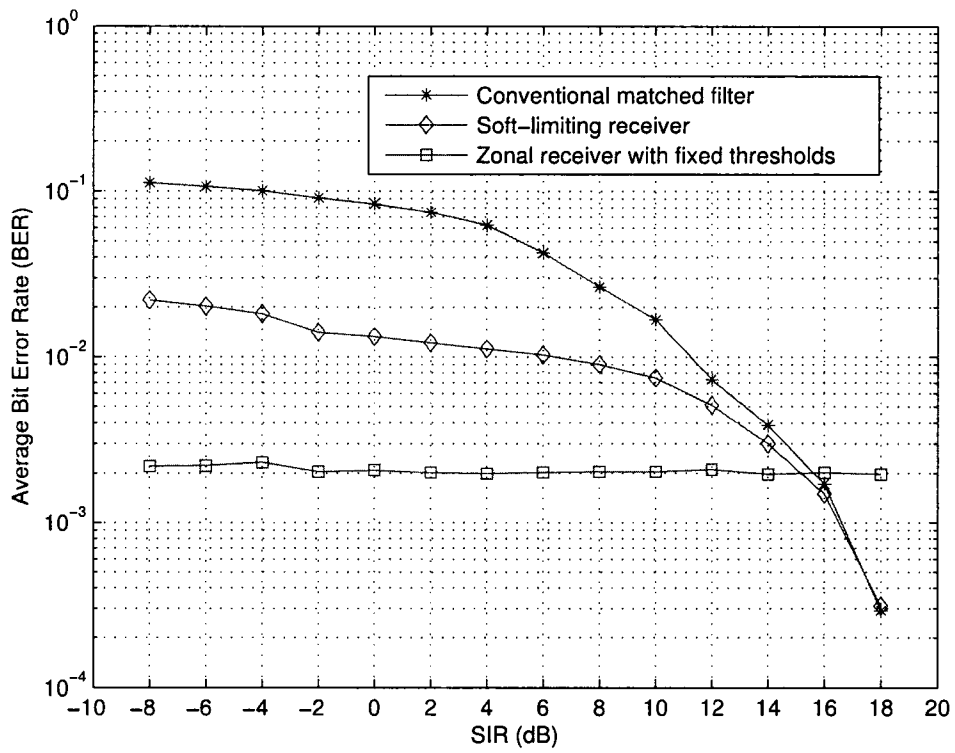


Fig. 4.6. The average BER versus SIR of the conventional matched filter UWB receiver, the soft-limiting UWB receiver and the zonal UWB receiver with fixed thresholds with $N_s=4$ and $N_u=4$ when only MAI is present.

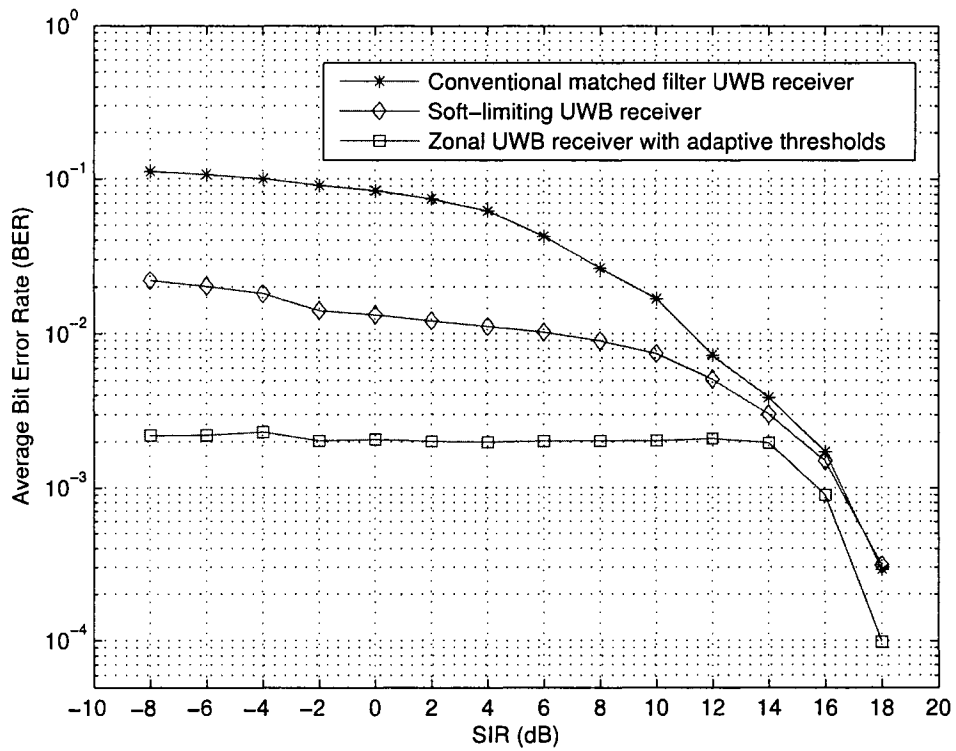


Fig. 4.7. The average BER versus SIR of the conventional matched filter UWB receiver, the soft-limiting UWB receiver and the zonal UWB receiver with adaptive thresholds with $N_s=4$ and $N_u=4$ when only MAI is present.

system as subsequent results will show. As the SIR becomes larger, the BER curve for the zonal receiver remains level while those of the conventional matched filter UWB receiver and the soft-limiting UWB receiver decrease rapidly and cross below the BER curve of the zonal receiver when the SIR exceeds 14 dB. The zonal receiver with fixed thresholds underperforms the conventional matched filter UWB receiver and the soft-limiting receiver for large values of SIR.

If we make the thresholds of the zonal receiver adaptive and use computer search to obtain the optimal lower and upper thresholds that minimize the BER, the zonal receiver must always meet or surpass the performance of the conventional matched filter UWB receiver. This is because, as stated previously, when lower threshold $t_l = 0$ and upper threshold $t_h = \infty$, the zonal receiver becomes the conventional matched filter UWB receiver. Some example BER curves for the conventional matched filter UWB receiver, the soft-limiting UWB receiver and the adaptive zonal receiver are shown in Fig. 4.7. It is seen that the zonal UWB receiver with adaptive thresholds outperforms both the conventional matched filter UWB receiver and the soft-limiting UWB receiver for all SIR values in this case. When the SIR is small, the performance gains are the same as those of the zonal receiver with fixed thresholds seen previously in Fig. 4.6. The gains decrease as the SIR increases. For example, when SIR = 18 dB, the zonal receiver with adaptive thresholds achieves 1/3 the BER of the conventional matched filter UWB receiver and the soft-limiting UWB receiver.

Although the zonal UWB receiver with fixed thresholds doesn't perform as well as

the zonal UWB receiver with adaptive thresholds and it underperforms the conventional matched filter UWB receiver and the soft-limiting UWB receiver when the SIR is large, it is still very useful because the structure is simple and easy to implement since no search is needed to obtain the optimal thresholds. The zonal UWB receiver with fixed thresholds can be used to effectively detect UWB signals when the SIR is less than 16 dB.

Fig. 4.8 shows the optimal lower and upper thresholds of the zonal UWB receiver for all SIR values in the example of Fig. 4.7. Some very interesting observations and conclusions follow from this figure. Note that in the SIR region $[-8 \text{ dB}, 14 \text{ dB}]$, the optimal lower threshold t_l and upper threshold t_h are well approximated by $S_m - 0.05$ and $S_m + 0.05$, respectively. Considering Figs. 4.1 and 4.2, and the associated discussion, it is to be expected that with the optimal lower and upper thresholds, (t_l, t_h) and $(-t_h, -t_l)$ will enclose small regions centered around S_m and $-S_m$. One can explain the near independence of (t_l, t_h) on SIR in the following way. In the interference-limited case, consider the statistics of the MAI to be fixed, and then increasing the SIR corresponds to increasing the value of $|S_m|$, or translating the conditional pdf of the MAI. Note that the distribution of r_m then remains the same in the region $(S_m - 0.05, S_m + 0.05)$. Hence, the probability that r_m falls into $(S_m - 0.05, S_m + 0.05)$ is not changing with the SIR in this case. This explains why the lower and upper thresholds of the zonal UWB receiver are well approximated by $S_m - 0.05$ and $S_m + 0.05$, and why the performance of the zonal UWB receiver with fixed thresholds $S_m - 0.05$ and $S_m + 0.05$ is almost constant (Fig. 4.6), and why the performance of the zonal UWB receiver with adaptive thresholds changes little as the SIR increases from -8

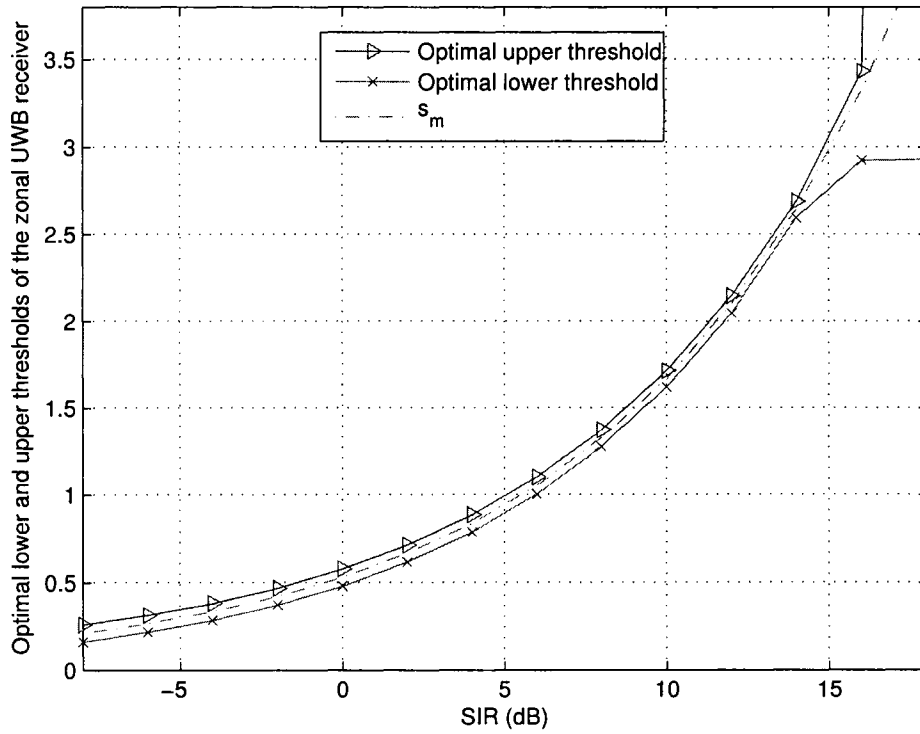


Fig. 4.8. The optimal lower and upper thresholds of the zonal UWB receiver with $N_s=4$ and $N_u=4$ when only MAI is present.

dB to 14 dB (Fig. 4.7). However, as the SIR becomes larger than 14 dB, the left tail of the conditional pdf $f(r_m|d_0^{(1)} = +1)$ moves increasingly above $r_m = 0$. Note that r_m , the amplitude of the chip correlator output has a lower bound and the pdf of r_m will be zero below this lower bound. This means that the performance of the zonal receiver with fixed thresholds will level off for large values of SIR. On the other hand, the BER curves for the conventional matched filter UWB receiver and the soft-limiting UWB receiver converge and decrease rapidly as the SIR increases above 14 dB. Therefore, the zonal UWB receiver with fixed thresholds will underperform the conventional matched filter UWB receiver and the soft-limiting UWB receiver for large values of SIR, which is shown by Fig. 4.6. However, the zonal receiver structure with adaptive lower and upper thresholds will outperform the other two receivers. Observe in Fig. 4.8 that both optimal lower and upper thresholds of the zonal UWB receiver move farther away from the value S_m as the SIR gets larger than 14 dB, which makes the zonal receiver structure similar to the conventional matched filter UWB receiver. Fig. 4.7 shows that, with optimal lower and upper thresholds, the zonal UWB receiver's BER performance improves with increasing SIR and surpasses those of the conventional matched filter UWB receiver and the soft-limiting UWB receiver.

4.4.2 Performance in mixed MAI and AWGN channels

Note that the zonal UWB receiver can achieve large gains for small values of SIR. However, such large gains cannot be achieved in practical environments where both MAI and AWGN are present. The BER of TH-BPSK systems with 3 interferers using the zonal UWB re-

ceiver are evaluated in this subsection as a function of SNR showing the BER performance of the newly proposed UWB receiver in mixed MAI and AWGN environments.

Fig. 4.9 shows the BER curves for the conventional matched filter UWB receiver, the adaptive threshold soft-limiting UWB receiver and the zonal UWB receiver with $N_s = 4$ and $N_u = 4$ for a value of SIR = 10 dB where both MAI and AWGN are present in the channel. Observe that when the SNR is small, i.e. the AWGN dominates the MAI, $Y_m = I_m + N_m$ can be approximated as Gaussian distributed RV, and the conventional matched filter UWB receiver works essentially as well as the optimal receiver [28]. Under such circumstances, the adaptive threshold soft-limiting UWB receiver and the zonal UWB receiver can adjust their thresholds to meet the BER performance of the conventional matched filter UWB receiver. But as the SNR gets large enough that the noise term stops dominating the MAI, the adaptive threshold soft-limiting UWB receiver and the zonal UWB receiver begin to outperform the conventional matched filter UWB receiver. Fig. 4.9 shows that in the SNR region [14 dB, 20 dB], both the adaptive threshold soft-limiting UWB receiver and the zonal UWB receiver with adaptive thresholds outperform the conventional matched filter UWB receiver, and the adaptive threshold soft-limiting receiver has a slightly better performance than the zonal receiver. After the SNR reaches 20 dB, the BER curves of the conventional matched filter UWB receiver and the adaptive threshold soft-limiting receiver both reach error rate floors before the zonal UWB receiver reaches an error floor. When the SIR = 10 dB, the error rate floor of the zonal UWB receiver is 1.8×10^{-3} , which is 10 times smaller than the error floor of the conventional matched filter UWB receiver (1.8×10^{-2}) and 4.1

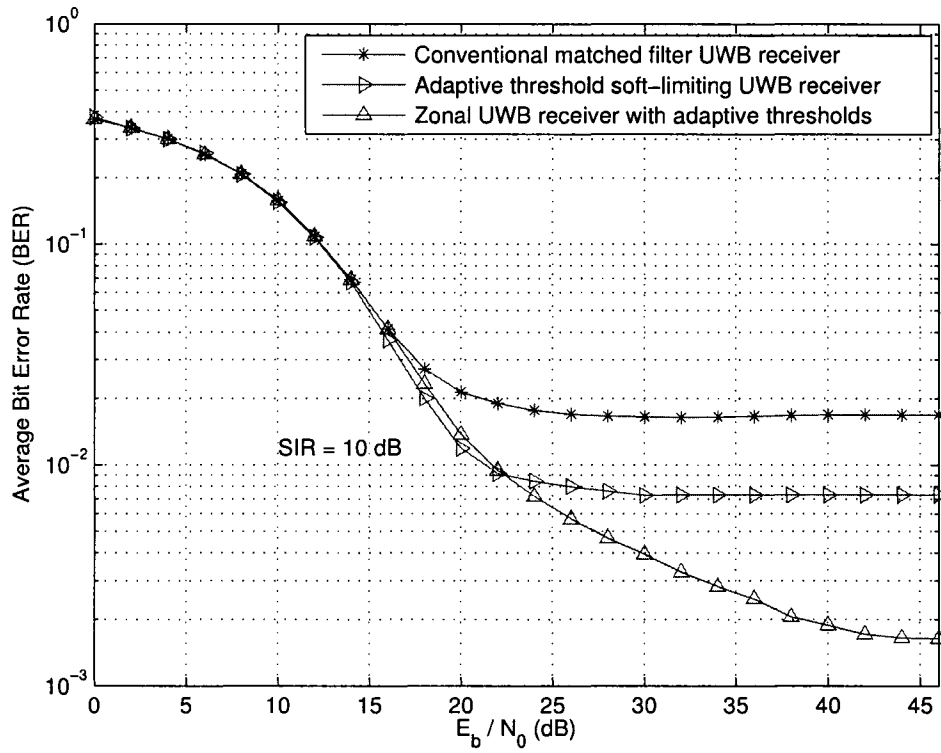


Fig. 4.9. The average BER versus SNR of the conventional matched filter UWB receiver, the adaptive threshold soft-limiting UWB receiver and the zonal UWB receiver with $N_s=4$ and $N_u=4$ when both MAI and AWGN are present.

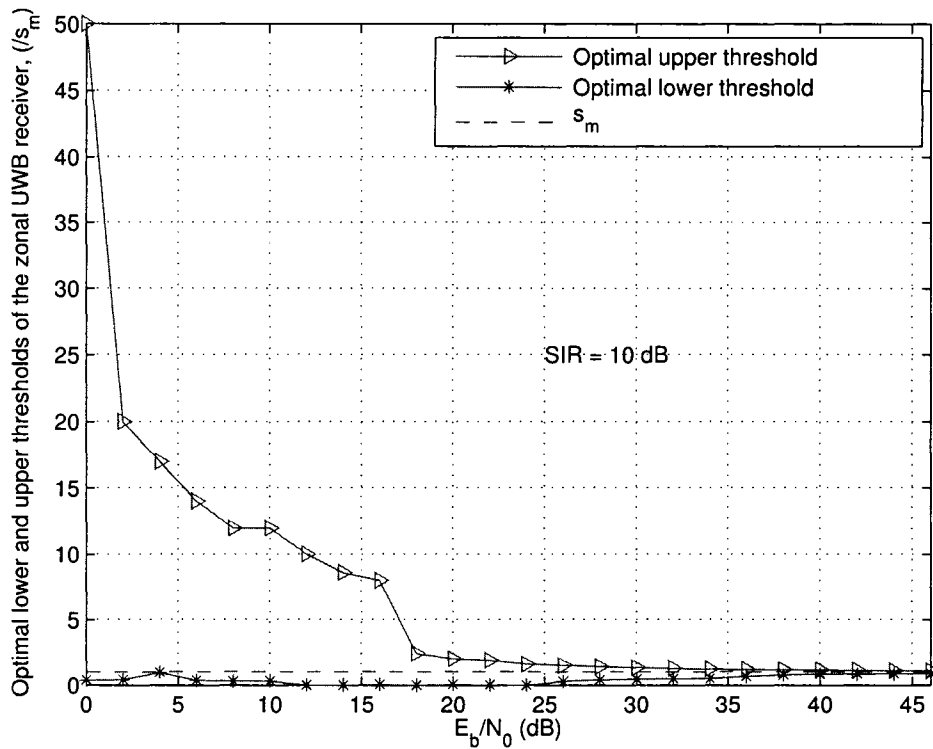


Fig. 4.10. The optimal lower and upper thresholds of the zonal receiver with $N_s=4$ and $N_u=4$ when both MAI and AWGN are present.

times smaller than that of the adaptive threshold soft-limiting UWB receiver (7.5×10^{-3}).

Fig. 4.10 shows the optimal lower and upper thresholds of the zonal UWB receiver with $N_s = 4$ and $N_u = 4$ for the example of Fig. 4.9. It is seen that, when the AWGN dominates the MAI, where $Y_m = I_m + N_m$ can be approximated as a Gaussian distributed RV, the optimal lower threshold of the zonal UWB receiver is close to zero and the upper threshold is large, which makes the zonal UWB receiver very similar to the conventional matched filter UWB receiver. As the SNR gets larger and the MAI becomes more significant in $Y_m = I_m + N_m$, the optimal lower and upper thresholds move towards S_m . When the SNR is large enough that the MAI dominates the AWGN, the optimal lower and upper threshold become close to S_m , and then the zonal UWB receiver structure is the same structure as first proposed for the case where only MAI is present in the channel.

4.5 Zonal Receiver Structure Design

In our analysis on the zonal UWB receiver design, the channel is assumed to be stable and time-invariant. That is because, for UWB systems, the bandwidth of the signal is very large, which is on the order of gigahertz, and the data rate of UWB systems is usually on the order of hundreds of megahertz. In this case, the transmission time is so short that UWB channels can be assumed to be static during the transmission time.

The analysis above shows how a zonal UWB receiver can be designed for a certain UWB systems. When the parameters of the UWB system are known, then simulations could be carried out to obtain the optimal thresholds of the zonal UWB receiver. Once the

thresholds are obtained, the values can be put into the zonal UWB receiver structure for the signal detection. Based on the fact that UWB channels can be assumed to be static during the transmission, one can say that, although the process of obtaining the optimal thresholds adds a bit of complexity to the receiver design, it is worth the cost since once the optimal thresholds are obtained, the zonal UWB receiver should always work well in the system.

4.6 Summary and Conclusions

In this chapter, a new UWB receiver structure dubbed the “zonal” receiver has been proposed based on observations of the pdf of the MAI in TH-UWB systems. It was shown to achieve better BER performance than the conventional matched filter UWB receiver and the soft-limiting UWB receiver for all SIR values when only MAI is present in the channel. In more practical environments where both MAI and AWGN are present, the zonal receiver always meets or outperforms the conventional matched filter UWB receiver. It achieves better performance than the adaptive threshold soft-limiting UWB receiver for large values of SNR.

Chapter 5

Conclusions and Future work

Gaussian approximations for the MAI have been widely adopted in UWB systems and the corresponding optimal receiver, the conventional matched filter UWB receiver was originally introduced and widely used in UWB systems. However, it is shown by many literatures on UWB system performance that the Gaussian approximation is not valid to predict the BER performance of UWB systems and it highly underestimates the BER of UWB systems. Other approximations for the MAI in UWB have been introduced and the corresponding optimal receiver structures have been derived. However, the actual pdf of the MAI in UWB systems is still unknown, therefore, there is no evidence showing any one of the existing receiver structures is the optimal receiver for UWB systems. On the other hand, although evaluating the actual pdf of the MAI has been proved cumbersome and it is not tractable to derive an optimal receiver structure based on the true pdf, a better receiver can still be designed based on observations of the simulated pdf of the MAI in UWB

systems, and on this basis, we have proposed a new receiver structure. The new receiver, dubbed the “zonal” UWB receiver, is shown to have superior performance in multiple access interference channels. In this chapter, the principal conclusions of our research will be enumerated, and problems that merit future research will be suggested.

5.1 Conclusions

1. When only MAI is present in UWB channels, the correlator output r_m can be expressed as $I_m + S_m$, where I_m and S_m are the MAI component and the desired signal component in the m th frame, respectively. The simulated pdf of the chip correlator output r_m in this case shows that there is an impulse at the point $r_m = S_m$ when the information bit +1 was transmitted and the impulse appears at the point $r_m = -S_m$ when the transmitted information bit was -1, as expected.
2. The simulated pdfs show that, if t_h and t_l assume certain values, in the region (t_l, t_h) , the conditional pdf of the chip correlator output r_m when the information bit +1 was sent, $f(r_m | d_0^{(1)} = +1)$, is as large or larger than the conditional pdf of r_m when the transmitted information bit is -1, $f(r_m | d_0^{(1)} = -1)$. On the other hand, in the region where $r_m \in (-t_h, -t_l)$, the conditional pdf $f(r_m | d_0^{(1)} = -1)$ is as large or larger than $f(r_m | d_0^{(1)} = +1)$. This implies that if r_m falls inside (t_l, t_h) , there is a relatively large probability that the transmitted information bit is +1, while if r_m falls inside $(-t_h, -t_l)$, the corresponding information bit is more likely to be -1.

3. Outside the two regions (t_l, t_h) and $(-t_h, -t_l)$, the conditional pdfs $f(r_m | d_0^{(1)} = +1)$ and $f(r_m | d_0^{(1)} = -1)$ are both small and almost the same as each other, thus if r_m falls outside these two regions, it is unreliable to use this information to decide the transmitted information bit as +1 or -1.
4. The new UWB receiver dubbed the “zonal” UWB receiver is derived intuitively based on observations of the simulated pdf. It uses the chip correlator output sample r_m unaltered and lets it contribute to the final receiver decision statistic when the sample falls into the region (t_l, t_h) or $(-t_h, -t_l)$. On the other hand, if r_m falls outside of these two regions, one can hardly discern which information bit was sent, and the zonal UWB receiver discards the sample and adds 0 to the final decision statistic in this case.
5. The design of the zonal receiver is intuitive and motivated by some important observations of the simulated pdf instead of evaluation of the exact pdf. Thus, there is no reason to believe that the zonal receiver is the optimal UWB receiver. However, if we set the lower threshold t_l to 0 and the upper threshold t_h to infinity, the zonal UWB receiver becomes exactly the conventional matched filter UWB receiver, which means if the thresholds of the zonal UWB receiver are optimally adopted, it should perform at least as well as the conventional matched filter UWB receiver.
6. Monte-Carlo simulation is used to estimate the BER of UWB systems. The simulation results show that the zonal UWB receiver with fixed threshold outperforms the

conventional matched filter UWB receiver and the recently proposed soft-limiting UWB receiver in pure MAI channels when the SIR is small. The performance levels off when the SIR gets larger and the zonal UWB receiver underperforms the conventional matched filter UWB receiver and the soft-limiting UWB receiver when the SIR is larger than 14 dB. However, the zonal UWB receiver with optimal thresholds always outperforms the conventional matched filter UWB receiver and the soft-limiting UWB receiver for all the SIR values. The performance gains are large in the region where the SIR is small, and decrease as the SIR gets larger.

7. Although it is shown that the zonal UWB receiver can achieve large performance gains in pure MAI channels, such large gains cannot be achieved with the presence of AWGN in MAI channels. In MAI-plus-AWGN environments, the simulation results show that the zonal UWB receiver always meets or outperforms the conventional matched filter UWB receiver and its BER performances are better than the recently proposed adaptive threshold soft-limiting UWB receiver in the region where the SNR is large.
8. In pure MAI channels, if computer search is used to obtain the optimal thresholds of the zonal UWB receiver, the optimal lower and upper thresholds enclose small regions centered around S_m and $-S_m$ when the SIR is small, which is the same as the expectation based on observations of the simulated pdf of the chip correlator output. When the SIR increases and the left tail of the conditional pdf $f(r_m | d_0^{(1)} = +1)$ moves increasingly above $r_m = 0$, the conventional matched filter UWB receiver

and the soft-limiting UWB receiver outperform the zonal UWB receiver with fixed thresholds. In this case, the optimal lower threshold t_l becomes close to 0 and the optimal upper threshold t_h becomes very large, which makes the zonal receiver structure similar to the conventional matched filter UWB receiver. With these optimal thresholds, the zonal UWB receiver outperforms both the conventional matched filter UWB receiver and the soft-limiting UWB receiver for all the values of SIR in pure MAI channels.

9. In more practical MAI-plus-AWGN channels, when the SNR is small, the AWGN term is dominant in the total disturbance. Thus, the total disturbance can be approximated by a Gaussian distributed RV, and the conventional matched filter UWB receiver should be the optimal receiver. In this case, the optimal lower threshold of the zonal UWB receiver is close to 0 and the optimal upper threshold is very large, which makes the structure of the zonal UWB receiver similar to the conventional matched filter UWB receiver. When the SNR gets larger and the AWGN term stops dominating the MAI, the total disturbance starts to show the characteristics of the MAI in the channel and cannot be approximated by a Gaussian distributed RV. In this case, the optimal lower and upper thresholds t_l and t_h of the zonal UWB receiver become very close to S_m , and the resultant receiver structure is the same as firstly proposed for the case where only MAI is present in the channel.

5.2 Future Work

1. In our work, some particular scenarios are not considered. For example, in pure MAI channels when the SIR is very small, the two regions (t_l, t_h) and $(-t_h, -t_l)$ may partially overlap with each other. It hasn't been considered in our work because with the values of SIR and SNR we considered, such a scenario didn't appear. However, if it does happen, some small modifications can be made to the zonal UWB receiver to assure its performance superiority.
2. Our design of the zonal UWB receiver is intuitive. It is only based on observations of the simulated pdf and the information of the exact pdf of the MAI in UWB systems is not considered. If more information can be extracted from the statistics of the true pdf of the MAI, receiver design principles of statistical communication theory can be applied to derive a new receiver structure. The corresponding receiver structure is surely to have better BER performance than the existing receivers.
3. Our design didn't consider the UWB receiver design in multipath fading channels. If multipath fading channels are considered, Rake receiver should be introduced for the signal detection. In each finger of the Rake receiver, a zonal UWB receiver can be adopted to improve the BER performance of the receiver. The performance of this new UWB receiver in multipath fading channel can be evaluated and compared to that of the traditional Rake receiver.

Vita

Hua Shao

Education

- 09/2005-Present University of Alberta, Canada
Master of Science: Electrical and Computer Engineering.
- 09/2000-07/2004 Peking University, P. R. China
Bachelor of Science: Electrical Engineering and Computer Science.

Working Experience

- 09/2005-Present University of Alberta, Canada
Research Assistant and Teaching Assistant.
- 09/2002-07/2004 Peking University, P. R. China
Research Assistant and Teaching Assistant.

Awards

- 2004 “May 4th” Scholarship, Peking University.
- 2003 Excellent Student Leader Award, Peking University.
- 2003 Guanghua Scholarship, Peking University.
- 2002 ESEC Scholarship, Educational Service Exchange with China.
- 2001 Guanghua Scholarship, Peking University.

Publication

- H. Shao and N. C. Beaulieu, “A novel zonal UWB receiver structure with improved performance in multiple access interference”, submitted to WCNC 2007.
- H. Shao and N. C. Beaulieu, “A novel zonal UWB receiver with superior performance”, submitted to IEEE Trans. Wireless Commun..

Report of Invention

- N. C. Beaulieu and H. Shao, *Zonal UWB Receiver*, Oct. 6, 2006.

References

- [1] R. Aiello and A. Batra, *Ultra Wideband Systems: Technologies and Applications*. Oxford: Newnes, 2006.
- [2] F. Nekoogar, *Ultra-Wideband Communications: Fundamentals and Applications*. Prentice Hall, 2005
- [3] M. Z. Win and R. A. Scholtz, "Ultra-Wide Bandwidth Time-Hopping Spread-Spectrum Impulse Radio for wireless Multiple-Access Communications," *IEEE Trans. Commun.*, vol. 48, pp. 679-691, Apr. 2000.
- [4] X. Chen and S. Kiaei, "Monocycles shapes for ultra wideband system," in *Proc. IEEE Conf. Ultra Wideband Systems and Technologies*, 2002, pp. 597-600.
- [5] L. B. Michael, M. Gahvami, and R. Kohno, "Multiple pulse generator for ultra-wideband communication using Hermite polynomial based orthogonal pulses," in *Proc. IEEE Conf. Ultra Wideband Systems and Technologies*, 2002, pp. 47-51.
- [6] B. Parr, B. Cho, K. Wallace, and Z. Ding, "A Novel ultra-wideband pulse design algorithm," *IEEE Commun. Lett.*, vol.7, pp. 219-221, May 2003.

- [7] S. Benedetto, G. De. Vincentiis, and A. Luvison, "Error probability in the presence of intersymbol interference and additive noise for multilevel digital signals," *IEEE Trans. Commun.*, vol. COM-21, pp. 181-190, Mar. 1973.
- [8] M. Hao and S. B. Wicker, "Performance evaluation of FSK and CPFSK optical communication systems: A stable and accurate method," *J. Lightwave Technol.*, vol.13, pp.1613-1623, Aug. 1995.
- [9] N. C. Beaulieu and B. Hu, "A Pulse Design Paradigm for Ultra-Wideband Communication Systems," *IEEE Trans. Wireless Commun.*, vol. 4, pp.1274-1278, June 2006.
- [10] B. Hu and N. C. Beaulieu, "Pulse Shapes for Ultrawideband Communication Systems," *IEEE Trans. Wireless Commun.*, vol.4, pp.1789-1797, July 2005.
- [11] F. Ramirez-Mireles, "Ultra-wideband SSMA using time hopping and M-ary PPM", *IEEE J. Sel. Areas Commun.*, vol. 19, pp. 1186-1197, June 2001.
- [12] J. R. Foerster, "The performance of a Direct-Sequence Spread Spectrum Ultra-Wideband System in the presence of multipath, narrowband interference and multiuser interference", in *Proc. 2002 IEEE conf. UWB Sys. and Tech.*, 2002, pp. 87-91.
- [13] A. Taha and K. M. Chugg, "A theoretical study on the effects of interference on UWB multiple access impulse radio," in *Proc. IEEE Asilomar Conf. on Signals, Systems and Computers*, 2002, pp. 728-732.

- [14] G. Durisi and G. Romano, "On the validity of Gaussian approximation to characterize the multiuser capacity of UWB TH-PPM," in *Proc. IEEE Conf. on Ultra Wideband Systems and Technologies*, 2002, pp. 157-161.
- [15] G. Durisi and S. Benedetto, "Performance Evaluation of TH-PPM UWB Systems in the Presence of Multiuser Interference," *IEEE Commun. Lett.*, vol. 7, pp. 224-226, 2003.
- [16] A. R. Forouzan, M. Nasiri-Kenari, and J. A. Salehi, "Performance analysis of ultra-wideband time-hopping code division multiple access systems: Uncoded and coded schemes", in *Proc. ICC*, 2001, pp. 3017-3021.
- [17] B. Hu and N. C. Beaulieu, "Exact bit error rate of TH-PPM UWB systems in the presence of multiple access interference," *IEEE Commun. Lett.*, vol. 7, pp. 572-574, Dec. 2003.
- [18] B. Hu and N. C. Beaulieu, "Accurate Evaluation of Multiple-Access Performance in TH-PPM and TH-BPSK UWB systems," *IEEE Trans. Commun.*, vol. 52, pp. 1758-1766, Oct. 2004.
- [19] B. Hu and N. C. Beaulieu, "Accurate performance evaluation for time-hopping and direct-sequence UWB systems," *IEEE Trans. Commun.*, vol. 53, pp. 1758-1766, June 2005.
- [20] G. H. Golub and J. H. Welsh, "Calculation of Gauss quadrature rules," *Math. Comput.*, vol. 23, pp. 221-230, Apr. 1969 .

- [21] S. Benedetto and E. Biglieri, *Principles of Digital Transmission With Wireless Applications*. New York: Kluwer Academic/Plenum, 1999.
- [22] M. Schwartz and L. Shaw, *Signal Processing: Discrete Spectral Analysis, Detection, and Estimation*. McGraw Hill, 1975.
- [23] M. W. Thompson and H. S. Chang, "Coherent Detection in Laplace Noise," *IEEE Trans. on AES*, vol. 30, Apr. 1994.
- [24] N. C. Beaulieu and B. Hu, "A Soft-limiting receiver structure for time-hopping UWB in multiple access interference," in *Proc. International Symposium on Spread Spectrum Techniques and Applications, ISSSTA, 2006*, pp. 417-421.
- [25] N. C. Beaulieu and B. Hu, "An Adaptive Threshold Soft-Limiting UWB Receiver with Improved Performance in Multiuser Interference", in *Proc. IEEE International Conference on Ultra-Wideband, ICUWB, 2006*, pp. 405-410.
- [26] C. E. Shannon, "A mathematical Theory of Communication", *The Bell System Technical Journal*, vol. 27, pp. 379-423, 623-656, July, October, 1948.
- [27] M. Sabattini, E. Masry and L. B. Milstein, "A non-Gaussian approach to the performance analysis of UWB TH-BPPM Systems," in *Proc. IEEE Conf. on Ultra Wide-band Systems and Technologies, 2003*, pp. 52-55.
- zzz
- [28] J. G. Proakis, *Digital Communications*. New York: McGraw-Hill, 1995.

[29] A. Papoulis, *The Fourier Integral and Its Applications*. New York: McGraw-Hill, 1962.

[30] V. S. Somayazulu, "Multiple access performance in UWB systems using time hopping versus direct sequence spreading," in *Proc. WCNC'2002*, 2002, pp. 522-525.